STUDIES OF THE DOUBLE-WEDGE AND BICONVEX AIRFOILS IN HYPERSONIC FLOW

Thesis by

William Stuart Wunch

In Partial Fulfillment of the Requirements

For the Degree of

Aeronautical Engineer

California Institute of Technology

Pasadena, California

1948

ACKNOWLEDGMENT

The author is deeply appreciative of the assistance that he has been privileged to receive during this past year from Mr. Allen E. Puckett in the preparation of this thesis. To his countless valuable suggestions and unstinting sacrifice of time, the author shall be forever indebted. He would also like to thank Dr. Homer J. Stewart for his many helpful words of advice.

INTRODUCTION AND SUMMARY

Through the development of the high altitude rocket interest has turned to the investigation of aerodynamic problems beyond the supersonic regime. This domain of speed has been termed hypersonic, meaning high Mach number flight in a homogeneous medium whose molecules describe negligible mean free paths with respect to a chosen characteristic dimension. The thesis presented given an extension of two-dimensional supersonic airfoil theory to attack the problem of getting aerodynamic coefficients for the double-wedge and biconvex airfoils.

The shock wave equations along with those for Prandtl-Meyer flow have been modified by making approximations based on the hypersonic Mach numbers. These equations have been used to treat the following three cases:

(A) The Mach angle is much less than the deflection angle.

(B) The Mach angle is much greater than the deflection angle.

(C) The Mach angle is of the same order of magnitude as the deflection angle.

A brief discussion is made of the assumptions involved in the development of each of these flows to show that they do not violate basic principles. The hypersonic approximations already mentioned are then applied to these equations. In case (A) formulas are derived giving a quick approximation to the

lift, drag, and moment coefficients. In case (B) formulas are found to be similar to those already obtained by the small perturbation method for supersonic flow. The results of case (C) show that a singular investigation must be made of each airfoil. The results of each of these cases are presented in the section titled "Applications to the Double-wedge and Biconvex Airfoils." Results for symmetrical double-wedge airfoils, whose maximum thicknesses are 10 per cent of the chord and are located at 25, 50, and 75 per cent of the chord, are plotted in the appendix.

TABLE OF CONTENTS

LIST OF FIGURES

I. AERODYNAMIC COEFFICIENTS

The lift, drag, and moment coefficients of the double-wedge airfoil are obtained in the following analysis by consideration of the static pressures acting over the airfoil (for the notation used, see Fig. 1). Separating the pressure force into components acting parallel and perpendicular to the velocity from infinity, one obtains the lift and drag forces per unit span as the following:

$$L = q_\infty \{-C_{p_1} c_1 \cos\theta_1 - C_{p_2} c_2 \cos\theta_2 + C_{p_3} c_3 \cos\theta_3 + C_{p_4} c_4 \cos\theta_4\} \quad (1)$$

$$D = q_\infty \{-C_{p_1} c_1 \sin\theta_1 - C_{p_2} c_2 \sin\theta_2 + C_{p_3} c_3 \sin\theta_3 + C_{p_4} c_4 \sin\theta_4\} \quad (2)$$

where c_i denotes the chord section over which the C_{p_i} acts. Making the small angle approximations

$$\sin\theta \doteq \theta \qquad \cos\theta \doteq 1$$

the lift and drag forces per unit span may be expressed in coefficient form

$$C_L = \frac{L}{q_\infty c} = -C_{p_1} c_1' - C_{p_2} c_2' + C_{p_3} c_3' + C_{p_4} c_4' \quad (3)$$

$$C_D = \frac{D}{q_\infty c} = -C_{p_1} c_1' \theta_1 - C_{p_2} c_2' \theta_2 + C_{p_3} c_3' \theta_3 + C_{p_4} c_4' \theta_4 \quad (4)$$

where c_i' is c_i/c. The pitching moment with respect to the leading edge may readily be obtained by a simple consideration of the airfoil geometry

$$M_{LE} = q_\infty \left\{-C_{p_1} \frac{c_1^2}{2} \cos\theta_1 - C_{p_2} c_2 \left(c_1 + \frac{c_2}{2}\right) \cos\theta_2 + C_{p_3} \frac{c_3^2}{2} \cos\theta_3 + C_{p_4} c_4 \left(c_3 + \frac{c_4}{2}\right) \cos\theta_4\right\} \quad (5)$$

Using the approximations made in equations (3) and (4), one obtains the pitching moment coefficient per unit span

$$C_{m_{LE}} = \frac{M_{LE}}{q_\infty c^2} = -C_{p_1}\frac{c_1'^2}{2} - C_{p_2}c_2'\left(c_1' + \frac{c_2'}{2}\right) + C_{p_3}\frac{c_3'^2}{2} + C_{p_4}c_4'\left(c_3' + \frac{c_4'}{2}\right) \quad (6)$$

The lift and drag coefficients for the biconvex airfoil may be expressed in similar form to that for the double-wedge airfoil. The lift and drag forces per unit span, considering only the pressure forces, are the following:

$$L = q_\infty \left\{ \int_{-c/2}^{c/2} C_{p_l} \cos\theta_l \, dx - \int_{-c/2}^{c/2} C_{p_u} \cos\theta_u \, dx \right\} \quad (7)$$

$$D = q_\infty \left\{ \int_{-c/2}^{c/2} C_{p_l} \sin\theta_l \, dx - \int_{-c/2}^{c/2} C_{p_u} \sin\theta_u \, dx \right\} \quad (8)$$

The subscript notation u denotes the upper surface; l, the lower surface. For small θ, i.e., small perturbation analysis, one obtains for the lift and drag coefficients

$$C_L = \frac{L}{q_\infty c} = \int_{-1/2}^{1/2} C_{p_l} \, d\frac{x}{c} - \int_{-1/2}^{1/2} C_{p_u} \, d\frac{x}{c} \quad (9)$$

$$C_D = \frac{D}{q_\infty c} = \int_{-1/2}^{1/2} C_{p_l}\theta_l \, d\frac{x}{c} - \int_{-1/2}^{1/2} C_{p_u}\theta_u \, d\frac{x}{c} \quad (10)$$

The moment of the biconvex airfoil acting about the leading edge, neglecting pressure drag effects, is the following:

$$M_{LE} = q_\infty \left\{ \int_{-c/2}^{c/2} C_{p_l}(x + c/2)\cos\theta_u \, dx - \int_{-c/2}^{c/2} C_{p_u}(x + c/2)\cos\theta_l \, dx \right\} \quad (11)$$

Expressed in coefficient form, one obtains

$$C_{m_{LE}} = \frac{M_{LE}}{q_\infty c^2} = \int_{-1/2}^{1/2} C_{p_l}\left(\frac{x}{c} + 1/2\right)d\frac{x}{c} - \int_{-1/2}^{1/2} C_{p_u}\left(\frac{x}{c} + 1/2\right)d\frac{x}{c} \quad (12)$$

where the same approximations as previously used are applied.

In order to determine the aerodynamic coefficients of these airfoils it is therefore necessary to determine their respective pressure coefficients. Owing to the nature of the flow over the surfaces of the double-wedge airfoil, its pressure coefficients may readily be determined. In

particular the pressure coefficients are constant along each surface owing to the continuity condition of parallel flow. Again using the notation of Fig. 1, one has

$$C_{p_i} = \frac{p_i - p_\infty}{\frac{\rho_\infty}{2} U_\infty^2} = \frac{2}{\gamma M_\infty^2}\left(\frac{p_i}{p_\infty} - 1\right) \qquad (13)$$

These pressure ratios, which are related to the aerodynamic coefficients in a manner already shown, are functions of the Mach number, the type of flow described, and the geometric characteristics of the airfoil.

The local pressure coefficient for the biconvex airfoil is defined similarly. These are related to the aerodynamic coefficients by means of equations (9), (10) and (12). Letting the primes indicate conditions behind the leading edge disturbance, one has

$$C_{p_u} = \frac{2}{\gamma M_\infty^2}\left(\frac{p_u}{p_u}, \frac{p_u'}{p_\infty} - 1\right) \qquad C_{p_l} = \frac{2}{\gamma M_\infty^2}\left(\frac{p_l}{p_l}, \frac{p_l'}{p_\infty} - 1\right) \qquad (14)$$

The one assumption made at this point is that the flow is irrotational throughout the region near the airfoil. This fact means that Mach waves originating at the surface are reflected from the shock wave in a manner so as not to strike the airfoil. In the case of the biconvex airfoil this assumption is not valid, so that the results obtained for it are incorrect to that extent, assumed small. To approach the problem considering this rotationality condition would complicate the problem considerably. Results of supersonic airfoil theory show that the effect of this rotationality on the aerodynamic coefficients is negligible; this assumption is carried throughout this thesis.

II. HYPERSONIC APPROXIMATION OF FLOW WITH SHOCK WAVES

Let us consider the equations of motion of flow through an oblique shock wave; these may be summarized by the following four equations:

$$\rho_{1n} U_{1n} = \rho_\infty U_{\infty n} \tag{15}$$

$$\rho_1 U_{1n} U_{1t} = \rho_\infty U_{\infty n} U_{\infty t} \tag{16}$$

$$p_1 + \rho_1 U_{1n}^2 = p_\infty + \rho_\infty U_{\infty n}^2 \tag{17}$$

$$\frac{\gamma}{\gamma-1}\frac{p_1}{\rho_1} + \frac{U_{1n}^2}{2} + \frac{U_{1t}^2}{2} = \frac{\gamma}{\gamma-1}\frac{p_\infty}{\rho_\infty} + \frac{U_{\infty n}^2}{2} + \frac{U_{\infty t}^2}{2} \tag{18}$$

The nomenclature used here is described in Fig. 2. Equation (15) is the continuity equation expressing the constancy of mass flow existing on both sides of the shock wave. Equation (16) expresses the conservation of tangential momentum across the shock wave; equation (17) expresses the conservation of momentum normal to the shock wave. Equation (18) states the energy relationship valid in the adiabatic flow through the shock wave. Two basic assumptions made at this point are the following:

(1) There is no dissociation of the gas.

(2) A perfect gas with constant specific heats is used.

It is from these equations one wishes to obtain a solution of the hypersonic flow conditions existing behind the shock wave created at the leading edge of the airfoils. In particular relationships between the static pressures, the Mach numbers, and the deflection angles through the shock wave are desired.

A fifth equation, the boundary condition to be met

at the surface of the airfoil, and for reasons of continuity throughout the region in the vicinity of a diamond (double-wedge) airfoil, is that

$$\tan \theta_1 = \frac{V_1}{U_1} \tag{19}$$

Reference 1 gives a complete development of these equations of motion, p. 52, using the shock wave angle as the principal flow paramter. The results of this analysis are the following:

$$U_1 = \frac{U_\infty}{1 + \tan \beta_1 \tan \theta_1} \tag{20}$$

$$V_1 = \frac{U_\infty \tan \theta_1}{1 + \tan \beta_1 \tan \theta_1} \tag{21}$$

which yield the deflection angle relationship

$$\frac{1}{M_\infty^2} = \sin^2 \beta_1 - \frac{\gamma+1}{2} \frac{\sin \beta_1 \sin \theta_1}{\cos(\beta_1 - \theta_1)} \tag{22}$$

The static pressure rise is given by

$$P_1 - P_\infty = \rho_\infty U_\infty^2 \frac{\sin \beta_1 \sin \theta_1}{\cos(\beta_1 - \theta_1)} \tag{23}$$

and the pressure ratio across the shock wave by

$$\frac{P_1}{P_\infty} = \frac{2\gamma}{\gamma+1} M_\infty^2 \sin^2 \beta_1 - \frac{\gamma-1}{\gamma+1} \tag{24}$$

The relationship between the Mach number before the shock wave to that after it is

$$M_1^2 = \frac{1 + \frac{\gamma-1}{2} M_\infty^2}{\gamma M_\infty^2 \sin^2 \beta_1 - \frac{\gamma-1}{2}} + \frac{M_\infty^2 \cos^2 \beta_1}{1 + \frac{\gamma-1}{2} M_\infty^2 \sin^2 \beta_1} \tag{25}$$

As the analysis is made for a perfect fluid, i.e., non-viscous, compressible, under atmospheric conditions, the low temperature problem encountered in the hypersonic wind tunnel is not faced.

Proceeding further, one may impose the following conditions regarding β_1 and θ_1, since for this analysis

these angles are considered to be small:

$$\sin\beta_1 \doteq \beta_1 \qquad \sin\theta_1 \doteq \theta_1$$
$$\cos\beta_1 \doteq 1-\frac{\beta_1^2}{2} \qquad \cos\theta_1 \doteq 1-\frac{\theta_1^2}{2} \tag{26}$$

Equations (22)---(25) then become

$$\frac{1}{M_\infty^2} = \beta_1^2 - \frac{\gamma+1}{2}\frac{\beta_1\theta_1}{1-(\beta_1-\theta_1)^2} \tag{22a}$$

$$P_1 - P_\infty = \rho_\infty U_\infty^2 \frac{\beta_1\theta_1}{1-(\beta_1-\theta_1)^2} \tag{23a}$$

$$\frac{P_1}{P_\infty} = \frac{2\gamma}{\gamma+1} M_\infty^2 \beta_1^2 - \frac{\gamma-1}{\gamma+1} \tag{24a}$$

$$M_1^2 = \frac{1+\frac{\gamma-1}{2}M_\infty^2}{\gamma M_\infty^2 \beta_1^2 - \frac{\gamma-1}{2}} + \frac{M_\infty^2(1-\beta_1^2)}{1+\frac{\gamma-1}{2}M_\infty^2\beta_1^2} \tag{25a}$$

The assumptions just made are regarded as valid throughout this paper.

From equation (22a) a relationship of M_∞, β_1, and θ_1 may be found to be (neglecting third and fourth order terms)

$$M_\infty \beta_1 = \frac{\gamma+1}{4} M_\infty \theta_1 + \sqrt{\left(\frac{\gamma+1}{4} M_\infty \theta_1\right)^2 + 1} \tag{27}$$

where the minus (-) sign before the square root sign is voided because there is no physical meaning to it.

It is now convenient to introduce the hypersonic approximations as noted in the Introduction. These may be classified in the three categories

$$\text{(A)}\ \frac{1}{M_\infty} \ll \theta_1 \ll 1$$
$$\text{(B)}\ \theta_1 \ll \frac{1}{M_\infty} \ll 1 \tag{28}$$
$$\text{(C)}\ \theta_1 = O\left(\frac{1}{M_\infty}\right) \ll 1$$

Physically, case (28A) is that for which the Mach angle is less than the deflection angle; case (28B), that for which the reverse is true; case (28C), that for which the Mach

angle is of the same order of magnitude as the deflection angle. In each case the angles involved are much less than one radian.

From condition (28A) equations (23a)---(27) become

$$\beta_1 = \frac{\gamma+1}{2}\theta_1 \tag{29}$$

$$P_1 - P_\infty = \frac{\rho_\infty U_\infty^2}{2}(\gamma+1)\theta_1^2 \tag{30}$$

$$\frac{P_1}{P_\infty} = \frac{\gamma}{2}(\gamma+1)\theta_1^2 M_\infty^2 \tag{31}$$

$$M_1^2 = \frac{2}{\gamma-1}\frac{1}{\gamma\theta_1^2} \tag{32}$$

These then are the shock wave relationships to be used when the condition $\frac{1}{M_\infty} << \theta_1 << 1$ exists.

From condition (28B) a similar set of equations arise giving the conditions through the shock wave. It may be noted that should equation (27) be approximated by

$$M_\infty \beta_1 = 1$$

in order to make this analysis, that this step would be equivalent to assuming only Mach waves exist, or that the shock wave lies along the Mach wave. The other relationships would verify this conclusion. In this analysis then equation (27) is not modified from its stated form. Equations (23a) ---(25a) yield the following results with this approximation:

$$P_1 - P_\infty = \rho_\infty U_\infty^2 \beta_1 \theta_1 \tag{33}$$

$$\frac{P_1}{P_\infty} = \gamma M_\infty \theta_1 + 1 \tag{34}$$

$$M_1^2 = M_\infty^2\left(1 - (\gamma-1)\frac{\theta_1}{\beta_1}\right) \doteq M_\infty^2 \tag{35}$$

These then are the shock wave relationships to be used when the condition $\theta_1 << \frac{1}{M_\infty} << 1$ exists.

The most interesting of the three cases to be studied is that stated by (28C). From the four shock wave relationships formulated with this assumption, equations (29)---(35) may readily be obtained. Again equation (27) is not modified. The other relationships become somewhat more difficult to handle; expressed by the function $M_\infty \theta_1$, they are

$$P_1 - P_\infty = \rho_\infty U_\infty^2 \beta_1 \theta_1 \tag{36}$$

$$\frac{P_1}{P_\infty} = 1 + \gamma M_\infty^2 \theta_1 \beta_1 \tag{37}$$

$$M_1^2 = \frac{M_\infty^2}{\gamma \frac{\gamma-1}{2} M_\infty^2 \theta_1^2 + 1 + (\gamma-1)\theta_1/\beta_1} \tag{38}$$

Equations (27), (36)---(38) complete the relationships to be derived for the shock wave for hypersonic flow for the original assumptions (28).

Several interesting conclusions may be drawn from equations (29)---(38). Equation (32) states that the Mach number following the shock is dependent only on the deflection angle for $\frac{1}{M_\infty} \ll \theta_1 \ll 1$, which means, considering the order of magnitude, that M_1 is much less than M_∞. Equations (30) and (31) show that the increase in static pressure through the shock wave to be proportional to the square of the deflection angle and independent of the Mach number in the form of a pressure coefficient. Equation (29) shows that in the limit the shock wave angle is dependent only on the deflection angle; this fact might have been surmised from equation (32).

Replacing M_∞ with $\sqrt{M_\infty^2 - 1}$ it may be noted that the functions given by equations (33)---(35) reduce to those obtained in the small perturbation analysis of supersonic flow. This

result, too, might have been expected from the order of magnitude analysis made.

Equations (36)---(38) form the combination of these other approximations. From the nature of the approximation it may be seen that on application to airfoil problems that for positive increasing angles of attack the solution on the upper surface will converge to case (28B) and on the lower surface will converge to case (28A). These relationships are seen to be more exact in a mathematical sense since all the principal terms have been retained. In general it may be said that they do not handle well analytically and that a singular investigation must be made of each airfoil.

III. HYPERSONIC APPROXIMATION TO PRANDTL-MEYER FLOW

To obtain flow relationships in continuous shock-free streams, one might first investigate the equations of motion in the physical plane using the hypersonic approximation (large Mach number) and using a thin body. As seen in Reference 4, there results the following non-linear partial differential equation:

$$-M_\infty^2\phi_{xx} - 2\frac{M_\infty^2}{a_\infty}\phi_y\phi_{xy} + \left[1-(\gamma-1)\frac{M_\infty^2}{a_\infty}\phi_x - \frac{\gamma+1}{2}\frac{1}{a_\infty^2}\phi_y^2\right]\phi_{yy} = 0 \quad (39)$$

Failing to establish a linear differential equation for hypersonic flow in this manner, one resorts to the use of the hodograph plane by means of which non-linear equations become linearized without the introduction of approximations. The problem introduced in this simplification is that of satisfying the boundary conditions. From this investigation there results the relationship

$$\frac{dW}{W} = \frac{d\theta}{\sqrt{M_\infty^2-1}} \quad (40)$$

where W = the absolute magnitude of the velocity

θ = the inclination of the velocity vector from the reference axis of polar coordinates in the hodograph plane

As yet no restrictions other than steady, irrotational motion have been placed on this equation, especially that large deflection angles are permitted. In its development $W=W(\theta)$ was an essential element as well as the restriction to Mach numbers greater than one. In short equation (40) describes Prandtl-Meyer flow, or expansion flow, in which the expansion is accomplished by Mach waves. One

has already seen that a shock wave accompanies a compressive flow, so that now the complete flow pattern may be described. In particular it may be thought that an infinitesimally weak oblique shock wave is a Mach wave. Conversely one may imagine, in a very loose fashion, a shock wave as the superposition of infinitely many Mach waves along one line. If however, the Mach waves are not superimposed, but spread out over a region, the resulting overall compression is isentropic (owing to the fact that the entropy change across a weak shock is a small quantity of higher order than the pressure change.) The reverse motion, expansion, is possible to a limited extent as shown by equation (40) to bend the flow around a corner by means of an infinite number of Mach waves. If this equation were applied to a compression process of large magnitude on the other hand, one would be neglecting a large increase in entropy, the resulting analysis being that much in error. This equation then relates the velocity vectors on the two sides of the expansion Mach waves in accordance with the equations of motion for irrotational flow. However, it is restated, no specifications have been made with respect to the pattern of the Mach waves in the physical plane.

The flow field described by equation (40) then essentially consists of two regions separated by a Mach wave, the downstream region being entirely dependent upon the upstream conditions. The velocity is constant in each region, the velocity discontinuity through the Mach wave being described by equation (40). This change in speed causes a change in Mach number; the dependence of the velocity upon the Mach

number is expressed by means of the energy equation

$$\left(\frac{W}{C}\right)^2 = \left(1+\frac{2}{\gamma-1}\frac{1}{M^2}\right)^{-1} \tag{41}$$

where c = the maximum velocity when the absolute temperature is zero. Using the notation of Reference 1, one obtains

$$\frac{2W}{C^2}dW = \frac{4}{\gamma-1}\frac{dM}{M^3}\left(1+\frac{2}{\gamma-1}\frac{1}{M^2}\right)^{-2} = \frac{4W^4}{C^4}\frac{1}{\gamma-1}\frac{dM}{M^3}$$

Making the hypersonic approximation, M is large, one obtains from equation (40)

$$d\theta = \frac{2}{\gamma-1}\frac{dM}{M^2}$$

Integration yields

$$\theta_1 - \theta_\infty = \frac{2}{\gamma-1}\left(\frac{1}{M_\infty} - \frac{1}{M_1}\right) \tag{42}$$

Letting the curved wall or corner become continuous, so that one may describe it as an infinite number of straight line segments in the case of the wall, leads us to the integration performed. It may be visualized that successive changes may occur about the curved surface, the flow conditions being prescribed by equation (42).

The relationship between the Mach number and the amount of turning expressed in equation (42) presupposes that both M_∞ and M_1 are of the order of hypersonic magnitudes. Although this fact certainly is valid in expanding flow only, it does not necessarily apply with a preceding intense shock wave, such as may occur when the airfoil is at a positive angle of attack along the under surface. With initial hypersonic flow equation (42) is valid without qualification when the upper surface has only Prandtl-Meyer flow along its entire length, no leading edge shock wave occurring.

For the sake of completeness the next section is included

here. With a heavy oblique shock wave occurring at the leading edge so that M_1 is not to be considered hypersonic, this last analysis must be modified to take supersonic Mach numbers into account. On finding the conditions existing directly behind the shock wave, one may modify the analysis accordingly. Starting with the conditions existing behind the shock wave, the Prandtl-Meyer flow behind it may be exactly expressed on integration of equation (40) to yield

$$2(\theta_1 - \theta_2) = \sqrt{\frac{\gamma+1}{\gamma-1}}\sin^{-1}\left\{\frac{2\sqrt{\beta^2-1}}{(2+(\gamma-1)M_2^2)(2+(\gamma-1)M_1^2)}\cdot\right.$$
$$\left.\left[(2\gamma-(\gamma-1)M_1^2)\sqrt{M_2^2-1}-(2\gamma-(\gamma-1)M_2^2)\sqrt{M_1^2-1}\right]\right\}$$
$$+\sin^{-1}\left\{\frac{2}{M_2^2M_1^2}\left[(M_1^2-2)\sqrt{M_2^2-1}-(M_2^2-2)\sqrt{M_1^2-1}\right]\right\} \quad (43)$$

The Mach number at which one enters the hypersonic regime may arbitrarily be established, from which it is possible to determine whether equation (42) or (43) is to be used for determining the Mach number in the event of a heavy shock wave preceding the Prandtl-Meyer expansion. From the Mach number relationship, the pressure ratios and hence the pressure coefficient may be determined.

Since the flow through a Prandtl-Meyer expansion is isentropic, it is possible to relate the pressure after expansion to the pressure before expansion in the following manner:

$$P_{STAG.\infty} = P_{STAG.1}$$

The energy equation yields

$$\frac{U^2}{2} + C_p T = C_p T_s$$

or

$$\frac{T_s}{T} = 1 + \frac{\gamma-1}{2}M^2$$

Using isentropic flow relationships, one finds

$$\frac{P_1}{P_\infty} = \frac{P_1}{P_{3_1}} \frac{P_{3\infty}}{P_\infty}$$

$$\frac{P_1}{P_\infty} = \left(\frac{T_1}{T_{3_1}} \cdot \frac{T_{3\infty}}{T_\infty}\right)^{\frac{\gamma}{\gamma-1}}$$

$$\frac{P_1}{P_\infty} = \left\{\left(1+\frac{\gamma-1}{2}M_\infty^2\right)\Big/\left(1+\frac{\gamma-1}{2}M_1^2\right)\right\}^{\frac{\gamma}{\gamma-1}}$$

$$\frac{P_1}{P_\infty} = \left\{\left(1+.2M_\infty^2\right)\Big/\left(1+.2M_1^2\right)\right\}^{\frac{\gamma}{\gamma-1}} \qquad (44)$$

Making the hypersonic approximation after expanding in series form, equation (44) becomes

$$\frac{P_1}{P_\infty} = \left(\frac{M_\infty}{M_1}\right)^{\frac{2\gamma}{\gamma-1}}\left\{1+\frac{2}{\gamma-1}\frac{\gamma}{\gamma-1}\left(\frac{1}{M_\infty^2}-\frac{1}{M_1^2}\right)+HO\right\} \doteq \left(\frac{M_\infty}{M_1}\right)^{\frac{2\gamma}{\gamma-1}} \qquad (45)$$

Thus for Prandtl-Meyer hypersonic flow the dependency of the pressure ratio on the Mach number is found.

Algebraically manipulating equation (42) to

$$M_1 = \frac{M_\infty}{1-M_\infty(\theta_1-\theta_\infty)\frac{\gamma-1}{2}}$$

one sees several very important conclusions to be drawn considering the conditions of relation (28). Specifically when $M_\infty(\theta_1-\theta_\infty) > \frac{2}{\gamma-1}$ the following Mach number, M_1, is seen to be infinite. This situation may occur with the restriction of (28C), would more frequently occur with that of (28A), and would not occur with that of (28B). These facts will be further emphasized in the section on the application of this work to airfoil theory.

IV. APPLICATIONS TO THE DOUBLE-WEDGE AND BICONVEX AIRFOILS

A. The double-wedge airfoil.

Let us specify that the airfoils investigated will be symmetrical with respect to the chord line. Hence, it will be necessary only to evaluate positive angles of attack. The principal parameters involved will then be the position and the value of the maximum thickness as those affecting the aerodynamic coefficients from a geometric viewpoint.

The first analysis will be made assuming condition (28A) is valid:

$$\frac{1}{M_\infty} \ll \theta \ll 1 \tag{28A}$$

Also, one must specify that

$$\alpha < \delta_1 \tag{46}$$

Condition (46) states that shock waves exist, starting at both the upper and lower surface leading edges. Again adopting the notation of Fig. 1, one obtains the following from equations (13) and (31):

$$C_{p_1} = (\gamma+1)\,\theta_1^2 \tag{47}$$

$$C_{p_3} = (\gamma+1)\,\theta_3^2 \tag{48}$$

Since Prandtl-Meyer expansion occurs to turn the flow prior to regions ② and ④, one uses equation (42) in conjunction with equation (32) to obtain from equation (45)

$$\frac{P_2}{P_1}\left\{1 - \sqrt{\frac{\gamma-1}{2\gamma}}\,\frac{\delta_1+\delta_2}{|\theta_1|}\right\}^{\frac{2\gamma}{\gamma-1}} = F_1 \tag{49}$$

$$\frac{P_4}{P_3} = \left\{1 - \sqrt{\frac{\gamma-1}{2\gamma}}\,\frac{\delta_3+\delta_4}{|\theta_3|}\right\}^{\frac{2\gamma}{\gamma-1}} = F_3 \tag{50}$$

Relations (49) and (50) are plotted in Fig. 3, where for values of $\frac{(\delta_i+\delta_i)}{|\theta_i|} \geq 2.65$, F is zero. However, for $\frac{\delta_1+\delta_2}{|\theta_1|} \geq 1.65$

or $\frac{\delta_3+\delta_4}{|\theta_3|} > 1.65$, both $\frac{P_2}{P_1}$ and $\frac{P_4}{P_3}$ are less than .001, or zero for this analysis. Manipulating these conditions, one has

$$\delta_2 + \alpha \geq .65(\delta_1 - \alpha) \tag{51}$$

$$\delta_4 - \alpha \geq .65(\delta_3 + \alpha) \tag{52}$$

Condition (51) holds for the upper surface; condition (52), the lower surface. At zero degrees angle of attack there results the following condition for which $\frac{P_2}{P_1}$ equals zero.

$$\delta_2 \geq .655\,\delta_1 \tag{53}$$

Using a thin airfoil so that δ_1 and δ_2 may be approximated by $\frac{t'}{2c'}$ and $\frac{t'}{2(1-c')}$, respectively, (similarly for the lower surface owing to the symmetry), one obtains the condition for which the maximum thickness point position must not be forward for $\frac{P_2}{P_1}$ to be zero.

$$c_1' \geq .65 c_2' \qquad \text{or} \qquad c_1' \geq .394 \tag{53a}$$

It may now be noted that a condition on the angle of attack variation for which this approximation is valid may be gained from equations (51) and (52), or just (52) since the airfoil goes through positive angles of attack only.

$$\alpha \leq .394(1.54\,\delta_4 - \delta_3) \tag{54}$$

Since $c_4' = 1 - c_3'$ relation (54) becomes

$$\alpha \leq .394\left(1.54\,\frac{t'}{1-c_3'} - \frac{t'}{c_3'}\right) \tag{54a}$$

Equations (46) and (54a) are shown as the limiting lines of region (I) in Fig. 4. Hence within region (I) one obtains the following:

$$C_{p_2} = \frac{2}{\gamma M_\infty^2}\left(0\,\frac{P_1}{P_\infty} - 1\right) \doteq 0 \tag{55}$$

$$C_{p_4} = \frac{2}{\gamma M_\infty^2}\left(0\,\frac{P_3}{P_\infty} - 1\right) \doteq 0 \tag{56}$$

Practically speaking, one may interpret conditions (55) and (56) as meaning that the rear surfaces of the airfoil do not

contribute to the aerodynamic properties of the airfoil when the maximum thickness point as a function of the thickness is greater than the values illustrated in Fig. 4.

The aerodynamic coefficients then become, on substitution of equations (47), (48), (55), and (56) into equations (3), (4), and (6),

$$C_L = 2(\gamma+1)\alpha t'$$
$$C_D = (\gamma+1)t'\left\{\left(\frac{t'}{2C'}\right)^2 + 3\alpha^2\right\} \qquad (57)$$
$$C_{m_{LE}} = (\gamma+1)t'C'\alpha$$

where $C_1' = C_3' = C'$, and $\delta_1 = \delta_3 = \frac{t'}{2C'}$. These functions form part of the graph in Fig. 5 where the maximum thickness point position is used as the principal parameter for three ten per cent thick airfoils. In Fig. 6 one finds the drag coefficient for zero degrees angles of attack as a function of the maximum thickness point and its value. From the standpoint of the performance characteristics it is readily seen that the thinnest airfoil with the maximum thickness at the trailing edge would be the most suitable for the flight condition

$$\frac{1}{M_\infty} << \theta << 1 \qquad (28A)$$

In Fig. 7 one finds the lift and pitching moment derivatives at zero degrees angle of attack as functions of the maximum thickness and its position, the values for c' < .394 being obtained from equations (62). From relations (57) one may see that the center of pressure position is located half way to the maximum thickness point from the leading edge.

From equation (51) one obtains similar equations to (54) and (54a).

$$\alpha \geq .394\left(\frac{t'}{C'} - 1.54\frac{t'}{1-C'}\right) \qquad (58)$$

$$\alpha \geq .394\,(\delta_1 - 1.54\,\delta_2) \tag{58a}$$

Equations (46), (54a), and (58a) are shown as the limiting lines of region (II) in Fig. 4. Since in this region one has no longer a negligible value for $\frac{p_4}{p_3}$, one uses equations (55) and (50), which yields

$$C_{p_4} = \frac{2}{\gamma M_\infty^2}\left(\frac{p_4}{p_3}\frac{p_3}{p_1} - 1\right) \doteq \frac{p_4}{p_3} C_{p_3} = F_3 C_{p_3} \tag{59}$$

Therefore, in addition to the values of the aerodynamic coefficients given by equations (57) one has

$$\begin{aligned} \Delta C_L &= (\gamma+1)(1-c')\left(\alpha + \frac{t'}{2c'}\right)^2 F_3 \\ \Delta C_D &= -(\gamma+1)\left(\alpha + \frac{t'}{2c'}\right)^2 \left(\frac{t'}{2} - \alpha(1-c')\right) F_3 \\ \Delta C_{m_{LE}} &= (\gamma+1)\,\frac{1-c'}{2}^2 \left(\alpha + \frac{t'}{2c'}\right)^2 F_3 \end{aligned} \tag{60}$$

where the following restrictions are met:

$$\frac{1}{M_\infty} \ll \theta \ll 1 \tag{28A}$$

$$\alpha < \delta_1 \tag{46}$$

$$\alpha \geq .394\,(1.54\,\delta_4 - \delta_3) \tag{54a}$$

$$\alpha \geq .394\,(\delta_1 - 1.54\,\delta_2) \tag{58a}$$

If relations (53a) and (58a) are violated, i.e., the maximum thickness point is too forward at too small an angle of attack, region (III) shown in Fig. 4, one must make a further revision of equations (57) similar to that taken for equations (60). This modification would account for a very heavy shock wave that would result in the existence of a good amount of static pressure on the aft surfaces. The limiting lines of this region have already been described. In region (III) one uses equation (49) and (50) to yield equation (59) and

$$C_{p_2} = \frac{2}{\gamma M_\infty^2}\left(\frac{P_2}{P_1}\frac{P_1}{P_\infty} - 1\right) \doteq \frac{2}{\gamma M_\infty^2}\frac{P_2}{P}\frac{P_1}{P_\infty} = F_1 C_{p_1} \qquad (61)$$

Again, in addition to the values of the aerodynamic coefficients given by equations (57) one has

$$\Delta C_L = (\gamma+1)(1-c')\left\{\left(\alpha+\frac{t'}{2c'}\right)^2 F_3 - \left(\frac{t'}{2c'}-\alpha\right)^2 F_1\right\}$$

$$\Delta C_D = \left\{\left(\alpha+\frac{t'}{2c'}\right)^2\left(\alpha(1-c')-\frac{t'}{2}\right)F_3 - F_1\left(\frac{t'}{2c'}-\alpha\right)^2\left(\frac{t'}{2}+\alpha(1-c')\right)\right\}(\gamma+1) \qquad (62)$$

$$\Delta C_{m_{LE}} = (\gamma+1)\frac{1-c'^2}{2}\left\{\left(\alpha+\frac{t'}{2c'}\right)^2 F_3 - \left(\frac{t'}{2c'}-\alpha\right)^2 F_1\right\}$$

where the following restrictions are met

$$\frac{1}{M_\infty} << \theta << 1 \qquad (28A)$$

$$\alpha < \delta_1 \qquad (46)$$

$$\alpha \leq .394(\delta_1 - 1.54\,\delta_2) \qquad (58a)$$

Equations (60) and (62) show a much greater increase in drag for the additional amount of lift obtained. The net effect on the pitching moment is to put the center of pressure further aft. This is seen in Fig. 5.

The condition of $\theta = \alpha\left(\frac{1}{M_\infty}\right)$ or $\alpha \to \delta_1$ is discussed later in this section on double-wedge airfoils.

In contrast to condition (46) let us examine now the flow conditions that will occur when

$$\alpha > \delta_1 \qquad (63)$$

One notes that Prandtl-Meyer flow will occur at the leading edge over the upper surface. Thus the previous analysis is modified in regions ① and ② of Fig. 1. The lower surface is the same as that already discussed, its conditions being analyzed from Fig. 4. If in region Ⅳ, one uses equations (48) and (56)

$$C_{p_3} = (\gamma+1)\theta_3^2 \qquad (48)$$

$$C_{p_4} = 0 \qquad (56)$$

If in region (V) , one uses equations (48) and (59)

$$C_{P_4} = F_3 C_{P_3} \tag{59}$$

For the upper surface (1) combining equations (42) and (45), one obtains

$$\frac{P_1}{P_\infty} = \left\{ 1 - \frac{\gamma-1}{2} M_\infty \theta_1 \right\}^{\frac{2\gamma}{\gamma-1}} \tag{64}$$

which is always seen to be less than the value one. In terms of the pressure coefficient it is seen that this term is of higher order in comparison with equation (48). The same conclusion is reached for surface (2). Hence one obtains for the two upper surfaces

$$C_{P_1} = 0 \tag{65}$$

$$C_{P_2} = 0 \tag{66}$$

and the aerodynamic coefficients become

$$\begin{aligned} C_L &= (\gamma+1)\left(\alpha + \frac{t'}{2c'}\right)^2 c' \\ C_D &= (\gamma+1)\left(\alpha + \frac{t'}{2c'}\right)^3 c' \\ C_{m_{LE}} &= (\gamma+1)\left(\alpha + \frac{t'}{2c'}\right)^2 \frac{c'^2}{2} \end{aligned} \tag{67}$$

for the conditions

$$\frac{1}{M_\infty} \ll \theta \ll 1 \tag{28A}$$

$$\alpha > \delta_1 \tag{63}$$

$$\alpha \leq .394\left(1.54\frac{t'}{c'} - \frac{t'}{1-c'}\right) \tag{54a}$$

or they become in addition to the values of (67)

$$\begin{aligned} \Delta C_L &= (\gamma+1)(1-c')\left(\alpha + \frac{t'}{2c'}\right)^2 F_3 \\ \Delta C_D &= (\gamma+1)\left(\alpha + \frac{t'}{2c'}\right)^2 F_3 \left(\alpha(1-c') - \frac{t'}{2}\right) \\ \Delta C_{m_{LE}} &= (\gamma+1)\frac{1-c'^2}{2}\left(\alpha + \frac{t'}{2c'}\right)^2 F_3 \end{aligned} \tag{68}$$

for the conditions

$$\frac{1}{M_\infty} \ll \theta \ll 1 \tag{28A}$$

$$\alpha > \delta_1 \tag{63}$$

$$\alpha > .394\,(1.54\,\delta_4 - \delta_3) \tag{54a}$$

$$\alpha > .394\,(\delta_1 - 1.54\,\delta_2) \tag{58a}$$

Hence it is seen that a variety of formulas may be developed to cope with the particular example. The general formulas for the lift, drag, and moment coefficients are expressed by equations (57) and (67) to which various terms are added to take pressure recovery terms into account. Obviously from the drag coefficient curves, Fig. 6, the best airfoil would have its maximum thickness point at the trailing edge, being as thin as possible, and operated below the leading edge angle δ_1 .

The second major analysis will be made for the conditions stated by relation (28B)

$$\theta \ll \frac{1}{M_\infty} \ll 1 \tag{28B}$$

These formulas are shown to be identical with those obtained from two-dimensional airfoil theory, except that M_∞ is replaced by $\sqrt{M_\infty^2 - 1}$. Accordingly from equations (13) and (34) one obtains for

$$\alpha < \delta_1 \tag{46}$$

$$C_{p_1} = -2\theta_1 / M_\infty \tag{69}$$

and

$$C_{p_3} = 2\theta_3 / M_\infty \tag{70}$$

In sections ② and ④ of Fig. 1, separated from sections ① and ③ respectively by Prandtl-Meyer flow, one gets from equations (13), (34), (42), and (45)

$$C_{p_2} = \frac{2}{\gamma M_\infty^2}\left(\frac{p_2}{p_1}\frac{p_1}{p_\infty} - 1\right)$$

$$C_{p_2} = \frac{2}{\gamma M_\infty^2}\left\{\left(1 - \frac{\gamma-1}{2} M_\infty (\delta_1 + \delta_2)\right)^{\frac{2\gamma}{\gamma-1}} (1 - \gamma M_\infty \theta_1) - 1\right\}$$

$$C_{p_2} \doteq -\frac{2}{M_\infty}\theta_2 \tag{71}$$

Similarly $$C_{p_4} \doteq \frac{2}{M_\infty}\theta_4 \tag{72}$$

The aerodynamic coefficients then become the following:

$$C_L = \frac{4\alpha}{M_\infty}$$

$$C_D = \frac{4\alpha^2}{M_\infty} + \frac{t'^2}{M_\infty C'(1-C')} \tag{73}$$

$$C_{m_{LE}} = \frac{2\alpha}{M_\infty}$$

Without going into the details it may easily be determined that the same coefficient formulas are developed when $\alpha > \delta$. From the isentropic Prandtl-Meyer flow formulas and with due consideration of sign conventions, these are obtained from equations (13), (42), and (45), the values of C_{p_1} and C_{p_2} being the same as those expressed in equations (69) and (71).

Accordingly the double-wedge airfoils all have the same characteristics for the initial assumption (28B)

$$\theta << \frac{1}{M_\infty} << 1 \tag{28B}$$

except for the drag, from which it is immediately apparent that $\delta_1 = \delta_2$ or $C' \doteq .5$ is a necessary condition for minimum drag. The center of pressure is accordingly located at the fifty per cent chord point. Too, flat plate formulas may be derived readily by modifying equation (73) only. Fig. 8 shows the additional drag due to thickness plotted against the maximum thickness position.

The third case to be investigated, stated by condition (28C)

$$\theta = O\left(\frac{1}{M_\infty}\right) << 1 \tag{28C}$$

for $$\alpha < \delta \tag{74}$$

shows that a singular analysis must be made of every airfoil whose aerodynamic coefficients are desired. From equations (13), (37), and (38) one has

$$C_{p_1} = \frac{2}{\gamma M_\infty^2}\left(\frac{p_1}{p_\infty} - 1\right)$$

$$C_{p_1} = \frac{\gamma+1}{2}\theta_1^2\left[1 + \sqrt{1 + \left(\frac{4}{\gamma+1}\frac{1}{M_\infty\theta_1}\right)^2}\right]$$

$$G(M_\infty\theta) = 1 + \sqrt{1 + \left(\frac{4}{\gamma+1}\frac{1}{M_\infty\theta}\right)^2}$$

$$C_{p_1} = \frac{\gamma+1}{2}\theta_1^2 G(M_\infty\theta_1) \qquad (75)$$

where $G(M_\infty\theta)$ is plotted in Fig. 9. Similarly

$$C_{p_3} = \frac{\gamma+1}{2}\theta_3^2 G(M_\infty\theta_3) \qquad (76)$$

From equations (13), (42), and (45), as well as (75) and (76) one obtains

$$C_{p_2} = \left(\frac{p_2}{p_1}\frac{p_1}{p_\infty} - 1\right)\frac{2}{\gamma M_\infty^2}$$

$$C_{p_2} = \frac{2}{\gamma M_\infty^2}\left\{\left(\frac{M_1}{M_2}\right)^{\frac{2\gamma}{\gamma-1}}\left[\frac{\gamma M_\infty^2}{2}\left(\frac{\gamma+1}{2}\theta_1^2 G(M\theta_1) + 1\right)\right] - 1\right\}$$

$$C_{p_2} = J_1\left(M_1(\delta_1+\delta_2)\right)\frac{\gamma+1}{2}\theta_1^2 G(M\theta_1) + \frac{2}{\gamma M_\infty^2}\left(J_1(M_\infty\delta_1+\delta_2) - 1\right)$$

$$C_{p_2} = J_1 C_{p_1} + \frac{2}{\gamma M_\infty^2}(J_1 - 1) \qquad (77)$$

where $$J_1(M_1, \delta_1+\delta_2) = \left\{1 - \frac{\gamma-1}{2}M_1(\delta_1+\delta_2)\right\}^{\frac{2\gamma}{\gamma-1}}$$

or $$J_1(M_\infty, \delta_1+\delta_2) = \left\{1 - \frac{\gamma-1}{2}HM_\infty(\delta_1+\delta_2)\right\}^{\frac{2\gamma}{\gamma-1}} \qquad (78)$$

and $$H = \frac{M_1}{M_\infty} = \frac{1}{\sqrt{1 + \frac{\gamma-1}{2}\left(\gamma M_\infty^2\theta_1^2 + \frac{\theta}{\gamma+1}\frac{1}{G}\right)}} \qquad (79)$$

The function $H(M\theta)$ is evaluated from equations (27) and (38) and is plotted in Fig. 9. Accordingly

$$C_{p_4} = J_3 C_{p_3} + \frac{2}{\gamma M_\infty^2}(J_3 - 1) \qquad (80)$$

The values of the pressure coefficients so obtained were then placed in equations (3)---(6) for $\alpha < \delta_1$ and $\theta = O\left(\frac{1}{M_\infty}\right) << 1$ for the following three airfoils:

		Pos'n Max. Thickness
10% thick	(a)	.25c

10% thick	(b)	.50c
	(c)	.75c

In the event condition (74) is violated, or

$$\alpha > \delta_1 \tag{81}$$

one sees that the flow, as previously, changes character over the upper surfaces from the initial shock wave to an initial Prandtl-Meyer flow expansion. From equations (42), (45), and (13) there results

$$C_{p_1} = \frac{2}{\gamma M_\infty^2}\left(\frac{p_1}{p_\infty} - 1\right) = \frac{2}{\gamma M_\infty^2}\left\{\left(\frac{M_\infty}{M_1}\right)^{\frac{2\gamma}{\gamma-1}} - 1\right\}$$

$$C_{p_1} = \frac{2}{\gamma M_\infty^2}\left\{\left(1 - \frac{\gamma-1}{2} M_\infty \theta_1\right)^{\frac{2\gamma}{\gamma-1}} - 1\right\}$$

$$K_1(M_\infty \theta_1) = \left(1 - \frac{\gamma-1}{2} M_\infty \theta_1\right)^{\frac{2\gamma}{\gamma-1}}$$

$$C_{p_1} = \frac{2}{\gamma M_\infty^2}\left\{K_1(M_\infty \theta_1) - 1\right\} \tag{82}$$

where, as discussed previously, $\frac{p_1}{p_\infty}$ approaches zero when $M_\infty \theta_1 > 2.40$. This condition may be rewritten

$$\alpha > \frac{2.40}{M_\infty} + \delta_1 = \frac{2.40}{M_\infty} + \frac{t'}{2c'} \tag{83}$$

Since the flow is considered to be isentropic, one has similar expressions for $\frac{p_2}{p_\infty}$.

$$C_{p_2} = \frac{2}{\gamma M_\infty^2}\left\{K_2(M_\infty \theta_2) - 1\right\} \tag{84}$$

$$\alpha > \frac{2.40}{M_\infty} - \delta_2 = \frac{2.40}{M_\infty} - \frac{t'}{2(1-c')} \tag{85}$$

The limiting lines described by equations (83) and (85) are plotted in Fig. 10. It is seen that operation in region (VI) means that a signifigant static pressure does not exist on surfaces ① and ② . If in region (VII) , a signifigant static pressure exists over region ① , but not ② , i.e., flow separation takes place before surface ② is reached. If in region (VIII) signifigant static pressures exist over both upper surfaces. The ordinate origin

$\frac{2.40}{M_\infty}$ in Fig. 10 primarily establishes the region in which the airfoil is situated. In general it may be noted that surface ② has no aerodynamic value or very little for positive angles of attack.

It is seen that a variety of formulas may be developed to handle the particular example. The gereral formulas for the lift, drag, and moment coefficients are stated in equations (86) and (87), where various parts will drop out depending upon the existing conditions. For $\alpha < \delta_1$, there results

$$C_L = -\frac{\gamma+1}{2}\theta_1^2 G(M_\infty\theta_1)\{C' + (1-C')J_1\} + \frac{2}{\gamma M_\infty^2}(1-C')(J_3 - J_1) + \frac{\gamma+1}{2}\theta_3^2 G(M_\infty\theta_3)\{C' + (1-C')J_3\}$$

$$C_D = -\frac{\gamma+1}{2}\theta_1^2 G(M_\infty\theta_1)\{C'\theta_1 + (1-C')J_1\theta_2\} + \frac{2}{\gamma M_\infty^2}(1-C')\theta_2 - \theta_4) + \frac{\gamma+1}{2}\theta_3^2 G(M_\infty\theta_3)\{C'\theta_3 + (1-C')J_3\theta_4\} + \frac{2}{\gamma M_\infty^2}(1-C')(J_3\theta_4 - J_1\theta_2) \qquad (86)$$

$$C_{m_{LE}} = -\frac{\gamma+1}{2}\theta_1^2 G(M_\infty\theta_1)\left\{\frac{C'^2}{2} + \frac{1-C'^2}{2}J_1\right\} + \frac{1-C'^2}{\gamma M_\infty^2}(J_3 - J_1) + \frac{\gamma+1}{2}\theta_3^2 G(M_\infty\theta_3)\left\{\frac{C'^2}{2} + \frac{1-C'^2}{2}J_3\right\}$$

For $\alpha > \delta_1$, these become

$$C_L = -\frac{2}{\gamma M_\infty^2}\left(C'K_1 + (1-C')K_2 - 1\right) + \frac{\gamma+1}{2}\theta_3^2 G(M_\infty\theta_3)\{C' + J_3(1-C')\} + \frac{2}{\gamma M_\infty^2}(J_3 - 1)(1-C')$$

$$C_D = \frac{2}{\gamma M_\infty^2}\left(C'K_1\theta_1 + (1-C')K_2\theta_2 - 2\alpha\right) + \frac{2}{\gamma M_\infty^2}(J_3-1)(1-C')\theta_4 + \frac{\gamma+1}{2}G(M_\infty\theta_3)\{C'\theta_3 - (1-C')J_3\theta_4\}\theta_3^2 \qquad (87)$$

$$C_{m_{LE}} = -\frac{2}{\gamma M_\infty^2}\left(C'^2K_1 + \frac{1-C'^2}{2}K_2 - 1\right) + \frac{(J_2-1)}{\gamma M_\infty^2}(1-C'^2) + \frac{\gamma+1}{2}\theta_3^2 G(M_\infty\theta_3)\left\{\frac{C'^2}{2} + J_3\frac{1-C'^2}{2}\right\}$$

$G(M\theta)$ is given by equation (75); J, by equation (78); K by equation (82).

The results of this investigation are shown in Fig. 11 for the aforementioned airfoils. It is seen that for a Mach number of ten, corresponding to the Mach wave lying along the surface of the airfoil with the maximum thickness at .50c, that the minimum drag is accomplished by the airfoil with the maximum thickness at .75c, or the one whose leading edge lies within the Mach cone. Owing to the intense shock wave that exists for the airfoil having the maximum thickness at .25c, and owing to the more continuous flow of case (c) (the maximum thickness at .75c), the slope of the lift curve for the foil with the maximum thickness at .50c is the least of the three. The visible break in the slope of the lift curve of this airfoil occurs as the Prandtl-Meyer flow starts over the upper surface. As for the moment coefficient about the leading edge, it seems quite reasonable to expect that airfoil (b) has the minimum amount of unstable pitching moment owing to the small recovery of pressure along the aft portions of its surface: i.e., the center of pressure position is further forward. Too, the airfoil whose leading surfaces are within the Mach cone shows the greatest moment about the leading edge because the increased static pressure due to the shock wave acts over a greater portion of its surface than the others; i. e., the center of pressure is further aft, half way or more to the maximum thickness point. Since the center of pressure position is nearly constant in each case, it seems that the most favorable airfoil, as before, would be the one with its maximum thickness position at the trailing edge, and as thin as structurally possible.

B. The biconvex airfoil.

Owing to the geometric nature of this type of airfoil, it is readily seen that Mach waves are generated along its entire surface to turn the flow continuously. These waves are reflected by the leading edge shock wave, causing this shock wave to turn about the airfoil and causing the flow in the neighborhood of the airfoil to become rotational. In this analysis these effects will be neglected so that 'simple' expressions may be derived for the aerodynamic characteristics. The principal effort will be to determine basic factors affecting the aerodynamic characteristics under conditions (28), rather than to compute the coefficients. A more exact method, but somewhat more tedious, would be the method of characteristics.

Let us approximate the circular arc airfoil by means of the differential equation

$$d\frac{x}{c} = \frac{q}{c}\,d\theta \tag{88}$$

where the nomenclature is described in Fig. 12. Integration yields

$$\theta_u = \frac{c}{q}\left(\frac{x}{c} + 1/2\right) \tag{89}$$

where the condition is imposed that θ_u is zero at x/c = - 1/2. It is apparent that this airfoil is symmetrical about both major and minor axes, that the principal parameters involved are the chord length and the radius of curvature, or the leading edge angle and the curvature.

In the case given by condition (28A)

$$\frac{1}{M_\infty} << \theta << 1 \tag{28A}$$

one has from equations (9) and (14)

$$C_{L_u} = -\int_{-1/2}^{1/2} C_{p_u}\, d\frac{x}{c} \tag{9}$$

where $$C_{P_u} = \frac{2}{\gamma M_\infty^2}\left(\frac{P_u}{P_u'}\frac{P_u'}{P_\infty} - 1\right) \tag{14}$$

the primed quantities denoting the conditions existing just after the leading edge disturbance. From equations (31) and (45) one obtains

$$\frac{P_u'}{P_\infty} = \frac{\gamma}{2}(\gamma+1)\,\theta_u'^2 M_\infty^2 \tag{31}$$

$$\frac{P_u}{P_u'} = \left(\frac{M_u'}{M_u}\right)^{\frac{2\gamma}{\gamma-1}} \tag{45}$$

On substitution of these equations and (42), equation (9) becomes

$$C_{L_u} = -\frac{2}{\gamma M_\infty^2}\int_{-1/2}^{1/2}\left\{\frac{P_u'}{P_\infty}\left(1-\frac{\gamma-1}{2}M_u'\theta_u\right)^{\frac{2\gamma}{\gamma-1}} - 1\right\} d\frac{x}{c} \tag{90}$$

or with the variable x/c replaced by $\frac{a\theta}{c}$ from equation (88)

$$C_{L_u} = -\frac{2}{\gamma M_\infty^2}\frac{a}{c}\int_0^{2\bar{\delta}}\left\{\frac{P_u'}{P_\infty}\left(1-\frac{\gamma-1}{2}M_u'\theta_u\right)^{\frac{2\gamma}{\gamma-1}} - 1\right\} d\theta \tag{90a}$$

Presently the integration is carried over the entire airfoil. However, owing to the very high Mach number, separation may occur before that is reached. This effect is discussed later. Eliminating higher order terms, one obtains

$$C_{L_u} = -\frac{\gamma+1}{3\gamma-1}\,\frac{(\delta-\alpha)^3}{2\delta}\sqrt{2\gamma(\gamma-1)}\left[1-\left(1-\sqrt{\frac{\gamma-1}{2\gamma}}\,\frac{2\bar{\delta}}{\delta-\alpha}\right)^{\frac{3\gamma-1}{\gamma-1}}\right] \tag{91}$$

A similar expression is easily derived for the lift coefficient of the lower surface.

$$C_{L_\ell} = \frac{\gamma+1}{3\gamma-1}\,\frac{(\delta+\alpha)^3}{2\delta}\sqrt{2\gamma(\gamma-1)}\left[1-\left(1-\sqrt{\frac{\gamma-1}{2\gamma}}\,\frac{2\bar{\delta}}{\delta+\alpha}\right)^{\frac{3\gamma-1}{\gamma-1}}\right] \tag{91a}$$

The lift coefficient for the airfoil becomes

$$C_L = \frac{\gamma+1}{3\gamma-1}\,\frac{\sqrt{2\gamma(\gamma-1)}}{2\delta}\left\{-(\delta-\alpha)^3\left[1-\left(1-\sqrt{\frac{\gamma-1}{2\gamma}}\,\frac{2\bar{\delta}}{\delta-\alpha}\right)^{\frac{3\gamma-1}{\gamma-1}}\right]\right.$$
$$\left.+(\delta+\alpha)^3\left[1-\left(1-\frac{2\bar{\delta}}{\delta+\alpha}\sqrt{\frac{\gamma-1}{2\gamma}}\right)^{\frac{3\gamma-1}{\gamma-1}}\right]\right\} \tag{92}$$

where $\alpha < \delta$.

In the same way the drag coefficient is obtained from equations (10), (14), (31), (42), (45), and (88)

$$C_{D_u} = -\frac{2}{\gamma M_\infty^2}\frac{Q}{C}\int_0^{2\bar{\delta}}\left\{\frac{P_u'}{P_\infty}\left(1-\frac{\gamma-1}{2}M_u'\theta_u\right)^{\frac{2\gamma}{\gamma-1}}\left(\theta_u'+\theta_u\right)d\theta_u \right. \quad (93)$$

Integration and an order of magnitude analysis yield

$$C_{D_u} = \frac{\gamma+1}{3\gamma-1}\frac{\gamma-1}{2\gamma-1}\frac{\gamma}{2\bar{\delta}}(\delta-\alpha)^4\left\{-1+(2\gamma-1)\sqrt{\frac{2}{\gamma(\gamma-1)}}\right.$$
$$\left.-\left(1-\sqrt{\frac{\gamma-1}{2\gamma}}\frac{2\bar{\delta}}{\delta-\alpha}\right)^{\frac{3\gamma-1}{\gamma-1}}\left(-1+(2\gamma-1)\sqrt{\frac{2}{\gamma(\gamma-1)}}-\frac{3\gamma-1}{\sqrt{2\gamma(\gamma-1)}}\frac{2\bar{\delta}}{\delta-\alpha}\right)\right\} \quad (94)$$

A similar expression is derived in the same manner for the drag coefficient of the lower surface, resulting in the following expression for the total drag coefficient:

$$C_D = \frac{\gamma+1}{3\gamma-1}\frac{\gamma-1}{2\gamma-1}\frac{\gamma}{2\bar{\delta}}\left\{2\left(-1+(2\gamma-1)\sqrt{\frac{2}{\gamma(\gamma-1)}}\right)(\alpha^4+6\alpha^2\delta^2+\delta^4)\right.$$
$$-(\delta-\alpha)^4\left(1-\sqrt{\frac{\gamma-1}{2\gamma}}\frac{2\bar{\delta}}{\delta-\alpha}\right)^{\frac{3\gamma-1}{\gamma-1}}\left(-1+(2\gamma-1)\sqrt{\frac{2}{\gamma(\gamma-1)}}-\frac{3\gamma-1}{\sqrt{2\gamma(\gamma-1)}}\frac{2\bar{\delta}}{\delta-\alpha}\right)$$
$$\left.-(\delta+\alpha)^4\left(1-\sqrt{\frac{\gamma-1}{2\gamma}}\frac{2\bar{\delta}}{\delta+\alpha}\right)^{\frac{3\gamma-1}{\gamma-1}}\left(-1+(2\gamma-1)\sqrt{\frac{2}{\gamma(\gamma-1)}}-\frac{3\gamma-1}{\sqrt{2\gamma(\gamma-1)}}\frac{2\bar{\delta}}{\delta+\alpha}\right)\right\} \quad (95)$$

In an analogous manner one also obtains the moment coefficient of the airfoil about the leading edge to be

$$C_{m_{LE}} = \frac{\gamma+1}{3\gamma-1}\frac{\gamma-1}{2\gamma-1}\frac{\gamma}{4\delta^2}\left\{2(\alpha^4+6\alpha^2\delta^2+\delta^4)\right.$$
$$-(\delta-\alpha)^4\left(1-\sqrt{\frac{\gamma-1}{2\gamma}}\frac{2\bar{\delta}}{\delta-\alpha}\right)^{\frac{3\gamma-1}{\gamma-1}}\left(1+\frac{3\gamma-1}{\sqrt{2\gamma(\gamma-1)}}\frac{2\bar{\delta}}{\delta-\alpha}\right)$$
$$\left.-(\delta+\alpha)^4\left(1-\sqrt{\frac{\gamma-1}{2\gamma}}\frac{2\bar{\delta}}{\delta+\alpha}\right)^{\frac{3\gamma-1}{\gamma-1}}\left(1+\frac{3\gamma-1}{\sqrt{2\gamma(\gamma-1)}}\frac{2\bar{\delta}}{\delta+\alpha}\right)\right\} \quad (96)$$

Let us now examine the term

$$\left(1-\frac{2\bar{\delta}}{\delta+\alpha}\sqrt{\frac{\gamma-1}{2\gamma}}\right)^{\frac{3\gamma-1}{\gamma-1}} \quad (97)$$

which occurs frequently enough to cause some thought as to simplification. As with the double-wedge airfoil, it may be readily determined that for

$$0<\alpha<.72\delta \quad (98)$$

term (97) becomes less than .01 and can be neglected. Too, since the term

$$\frac{2\bar{\delta}}{\delta-\alpha} \quad (99)$$

is always greater or equal to that of term (98), it is seen that

$$\left(1-\frac{2\bar{\delta}}{\delta-\alpha}\sqrt{\frac{\gamma-1}{2\gamma}}\right)^{\frac{3\gamma-1}{\gamma-1}} \quad (97a)$$

becomes negligible for the condition (98). Accordingly the lift coefficient is modified

$$C_L = \frac{\gamma+1}{3\gamma-1}\frac{\sqrt{2\delta(\gamma-1)}}{\delta}(\alpha^3+3\alpha\delta^2) \tag{100}$$

for the condition

$$0<\alpha<.72\,\delta \tag{98}$$

A similar examination of the terms

$$\left(1-\sqrt{\frac{\gamma-1}{2\gamma}}\frac{2\delta}{\delta+\alpha}\right)^{\frac{3\gamma-1}{\gamma-1}}\left(-1+(2\gamma-1)\sqrt{\frac{2}{\gamma(\gamma-1)}}-\frac{3\gamma-1}{\sqrt{2\delta(\gamma-1)}}\frac{2\delta}{\delta+\alpha}\right) \tag{101}$$

shows that for

$$0<\alpha<.66\,\delta \tag{102}$$

these terms too may be neglected. Since the term

$$\left(1-\sqrt{\frac{\gamma-1}{2\gamma}}\frac{2\delta}{\delta-\alpha}\right)^{\frac{3\gamma-1}{\gamma-1}}\left(-1+(2\gamma-1)\sqrt{\frac{2}{\gamma(\gamma-1)}}-\frac{3\gamma-1}{\sqrt{2\delta(\gamma-1)}}\frac{2\delta}{\delta-\alpha}\right) \tag{101a}$$

is always less than (101) for positive angles of attack, this term may always be neglected. The drag coefficient then becomes

$$C_D = \frac{\gamma+1}{3\gamma-1}\frac{\gamma-1}{2\gamma-1}\frac{\gamma}{\delta}\left(-1+(2\gamma-1)\sqrt{\frac{2}{\gamma(\gamma-1)}}\right)(\alpha^4+6\alpha^2\delta^2+\delta^4) \tag{103}$$

for the condition

$$0<\alpha<.66\,\delta \tag{102}$$

The terms

$$\left(1-\sqrt{\frac{\gamma-1}{2\gamma}}\frac{2\delta}{\delta+\alpha}\right)^{\frac{3\gamma-1}{\gamma-1}}\left(1+\frac{3\gamma-1}{\sqrt{2\delta(\gamma-1)}}\frac{2\delta}{\delta+\alpha}\right) \tag{104}$$

appearing in the moment equation yield to a similar analysis the following information:

$$C_{m_{LE}} = \frac{\gamma+1}{3\gamma-1}\frac{\gamma-1}{2\gamma-1}\frac{\gamma}{2\delta^2}\left\{\alpha^4+6\alpha^2\delta^2+\delta^4\right\} \tag{105}$$

for the condition

$$0<\alpha<.38\,\delta \tag{106}$$

In the event that the restrictions imposed upon equations (100), (103), and (105) by (98), (102), and (106), respectively, are not valid for the positive angles of

attack, one obtains the following increments for the coefficients

$$\Delta C_L = \frac{\gamma+1}{3\gamma-1}\frac{\sqrt{2\gamma(\gamma-1)}}{2\delta}(\alpha+\delta)^3\left(1-\frac{2\bar{\delta}}{\delta+\alpha}\sqrt{\frac{\gamma-1}{2\gamma}}\right)^{\frac{3\gamma-1}{\gamma-1}} \tag{107}$$

for the condition

$$.72\,\delta < \alpha < \delta \tag{108}$$

$$\Delta C_D = -\frac{\gamma+1}{3\gamma-1}\frac{\gamma-1}{2\gamma-1}\frac{\gamma}{2\delta}(\delta+\alpha)^4\left(1-\sqrt{\frac{\gamma-1}{2\gamma}}\frac{2\bar{\delta}}{\delta+\alpha}\right)^{\frac{3\gamma-1}{2\gamma-1}}\left(-1+(2\gamma-1)\sqrt{\frac{2}{\gamma(\gamma-1)}}-\frac{(3\gamma-1)\,2\bar{\delta}}{\sqrt{2\gamma(\gamma-1)}\,\delta+\alpha}\right) \tag{109}$$

for the condition

$$.66\,\delta < \alpha < \delta \tag{110}$$

$$\Delta C_{m_{LE}} = -\frac{\gamma+1}{3\gamma-1}\frac{\gamma-1}{2\gamma-1}\frac{\gamma}{4\delta^2}(\delta+\alpha)^4\left(1-\sqrt{\frac{\gamma-1}{2\gamma}}\frac{2\bar{\delta}}{\delta+\alpha}\right)^{\frac{3\gamma-1}{2\gamma-1}}\left(1+\frac{3\gamma-1}{\sqrt{2\gamma(\gamma-1)}}\frac{2\bar{\delta}}{\delta+\alpha}\right) \tag{111}$$

for the condition

$$.38\,\delta < \alpha < \delta \tag{112}$$

It may now be observed that should flow separation take place before the trailing edge of the airfoil has been reached that the limits imposed on equations (100), (103), and (105) are lowered. As a function of the angle of separation, these limits are shown in Fig. 13 for the lift, drag, and moment coefficients. If these limits are exceeded, formulas (107), (109), and (111) are added to (100), (103), and (105), respectively, where $2\bar{\delta}$ is replaced by θ_{SEP}. The separation angle is determined from condition (97) set equal to .01.

One may next wish to investigate the conditions

$$\frac{1}{M_\infty} << \theta << 1 \tag{28A}$$

$$\alpha > \delta \tag{63}$$

A brief analysis of the lift coefficient for the upper surface will show that only higher order terms are involved. Again this amounts to a great simplification of the coefficients. From equations (9), (14), and (45) one has

$$C_{L_u} = \frac{2}{\gamma M_\infty^2}\int_{-1/2}^{1/2}\left\{\left(\frac{M_u'}{M_u}\right)^{\frac{2\gamma}{\gamma-1}}\frac{P_u'}{P_\infty}-1\right\}d\frac{x}{c}$$

Substituting equations (42) and (88), and integrating, one

obtains

$$C_{L_u} = \frac{2}{\gamma M_\infty^2} \frac{1}{2\bar{\delta}} \left\{ \frac{2}{3\gamma-1} \frac{P_u'}{P_\infty} \frac{1}{M_u'} \left(1 - \left(1 - \frac{\gamma-1}{2} M_u' 2\bar{\delta} \right)^{\frac{3\gamma-1}{\gamma-1}} \right) - 2\bar{\delta} \right\} \quad (113)$$

Because of the Prandtl-Meyer expansion at the leading edge, $\frac{P_u'}{P_\infty}$ is less than unity. But the principal factor leading to the higher order of magnitude of equation (113) is $\frac{1}{M_u'}$, which has a smaller value than $\frac{1}{M_\infty}$ due to flow expansion. This makes equation (113) a full order of approximation higher than those of equation (94), so that we may conclude

$$C_{L_u} = 0 \quad (114)$$

for

$$\alpha > \delta \quad (63)$$

A similar analysis will yield the facts that

$$C_{D_u} = 0 \quad (115)$$

$$C_{m_{u_{LE}}} = 0 \quad (116)$$

for condition (63). Therefore the aerodynamic coefficients become

$$C_L = \frac{\gamma+1}{3\gamma-1} \frac{\sqrt{2\gamma(\gamma-1)}}{2\bar{\delta}} (\alpha+\delta)^3 \left\{ 1 - \left(1 - \frac{2\bar{\delta}}{\delta+\alpha} \sqrt{\frac{\gamma-1}{2\gamma}} \right)^{\frac{3\gamma-1}{\gamma-1}} \right\}$$

$$C_D = \frac{\gamma+1}{3\gamma-1} \frac{\gamma-1}{2\gamma-1} \frac{\gamma}{2\bar{\delta}} (\alpha+\delta)^4 \left\{ 1 + (2\gamma-1)\sqrt{\frac{2}{\gamma(\gamma-1)}} - \left(1 - \sqrt{\frac{\gamma-1}{2\gamma}} \frac{2\bar{\delta}}{\delta+\alpha} \right)^{\frac{3\gamma-1}{\gamma-1}} \left(1 + (2\gamma-1)\sqrt{\frac{2}{\gamma(\gamma-1)}} + \frac{3\gamma-1}{\sqrt{2\gamma(\gamma-1)}} \frac{2\bar{\delta}}{\delta+\alpha} \right) \right\} \quad (117)$$

$$C_{m_{LE}} = \frac{\gamma+1}{3\gamma-1} \frac{\gamma-1}{2\gamma-1} \frac{\gamma}{4\bar{\delta}^2} (\alpha+\delta)^4 \left\{ 1 - \left(1 - \sqrt{\frac{\gamma-1}{2\gamma}} \frac{2\bar{\delta}}{\delta+\alpha} \right)^{\frac{3\gamma-1}{\gamma-1}} \cdot \left(1 + \frac{3\gamma-1}{\sqrt{2\gamma(\gamma-1)}} \frac{2\bar{\delta}}{\delta+\alpha} \right) \right\}$$

for the condition

$$\alpha > \delta \quad (63)$$

A short investigation of equations (103), (109), and (117) yields the fact that the main parameter affecting the quality of the airfoil will be δ, the opening angle of the airfoil. Translated into terms of thickness, one

deduces the expected result that the airfoil should be as thin as possible for maximum performance, i.e., minimum drag. In particular it may be derived that

$$2\delta = \frac{c}{q} = 4\,t/c \tag{118}$$

which may be substituted in previous expression if so desired.

In the case given by condition (28B)

$$\theta << \frac{1}{M_\infty} << 1 \tag{28B}$$

one obtains a similar analysis as that just presented. From equations (9), (14), (42), (35), and (45) there comes

$$C_{L_u} = \frac{2}{\gamma M_\infty^2} \int_{-1/2}^{1/2} \left\{ \frac{p_u'}{p_\infty} (1 - \gamma M_u' \theta_u) - 1 \right\} d\frac{x}{c} \tag{119}$$

where the approximation has been made

$$\left(1 - \frac{\gamma-1}{2} M_u' \theta_u\right)^{\frac{2\gamma}{\gamma-1}} \doteq (1 - \gamma M_u' \theta_u) \tag{120}$$

Substituting equation (88), one gets

$$C_{L_u} = \frac{2}{\gamma M_\infty^2} \frac{a}{c} \int_0^{2\delta} \left\{ \frac{p_u'}{p_\infty} (1 - \gamma M_u' \theta_u) - 1 \right\} d\theta_u \tag{119a}$$

As the Mach number is much lower than that discussed in the last section, the possibility of separation is not discussed here. Eliminating higher order terms, integration yields

$$C_{L_u} = \frac{2}{M_\infty} \alpha \tag{121}$$

A similar expression is derived for the lift coefficient of the lower surface, so that as with the double-wedge airfoil, one obtains

$$C_L = \frac{4\alpha}{M_\infty} \tag{122}$$

The analysis for the drag coefficient is conducted in the same manner. Similar to equation (119a) there is for the drag coefficient the following integral:

$$C_{D_u} = \frac{2}{\gamma M_\infty^2} \frac{a}{c} \int_0^{2\delta} \left\{ \frac{p_u'}{p_\infty} (1 - \gamma M_u' \theta_u) - 1 \right\} (\theta_u + \theta_u') \, d\theta_u \tag{123}$$

and a similar integral for the drag coefficients of the lower surface. These yield the well-known result for biconvex airfoils

$$C_D = \frac{4\alpha^2}{M_\infty} + \frac{4\delta^2}{3M_\infty} \tag{124}$$

or

$$C_D = \frac{4\alpha^2}{M_\infty} + \frac{16}{3}\frac{t'^2}{M_\infty} \tag{124a}$$

The integration of the moment coefficient equation for the upper surface

$$C_{mu} = \frac{2}{\gamma M_\infty^2}\frac{Q^2}{C^2}\int_0^{2\bar{\delta}}\left\{\frac{P_u}{P_\infty}'(1-\gamma M_\infty\theta_u)\,\theta_u\,d\theta_u \right. \tag{125}$$

obtained in the same manner as equations (119a) and (123), is readily performed. Added to the moment coefficient derived for the lower surface, one obtains the expected result

$$C_m = \frac{2\alpha}{M_\infty} \tag{126}$$

The formulas (122), (124), and (126) may be obtained from the small perturbation analysis of supersonic flow, M_∞ being replaced by $\sqrt{M_\infty^2-1}$. These formulas are not modified for the condition

$$\alpha > \delta$$

Again the importance of using a thin airfoil is apparent. The lift coefficient and the moment coefficient are seen to be independent of the shape of the airfoil.

The problem of the biconvex airfoil in the flow given by condition (28C)

$$\theta = O\left(\frac{1}{M_\infty}\right) << 1 \tag{28C}$$

may also be solved by the equations derived in this report.

REFERENCES

1. Liepmann, H. W., A. E. Ruckett; AERODYNAMICS OF A COMPRESSIBLE FLUID. John Wiley & Sons, Inc., New York, (1947).

2. Sauer, R.; THEORETICAL GAS DYNAMICS. Ed., J. W. Edwards, Ann Arbor, (1947).

3. von Karman, T.; Notes--Columbia University Lectures on Aerothermodynamics. Ed., William Perl, (1947).

4. Tsien, H-S.; "Similarity Laws of Hypersonic Flows," Journal of Mathematics and Physics. Vol. 25, No. 3, (October 1946).

APPENDIX

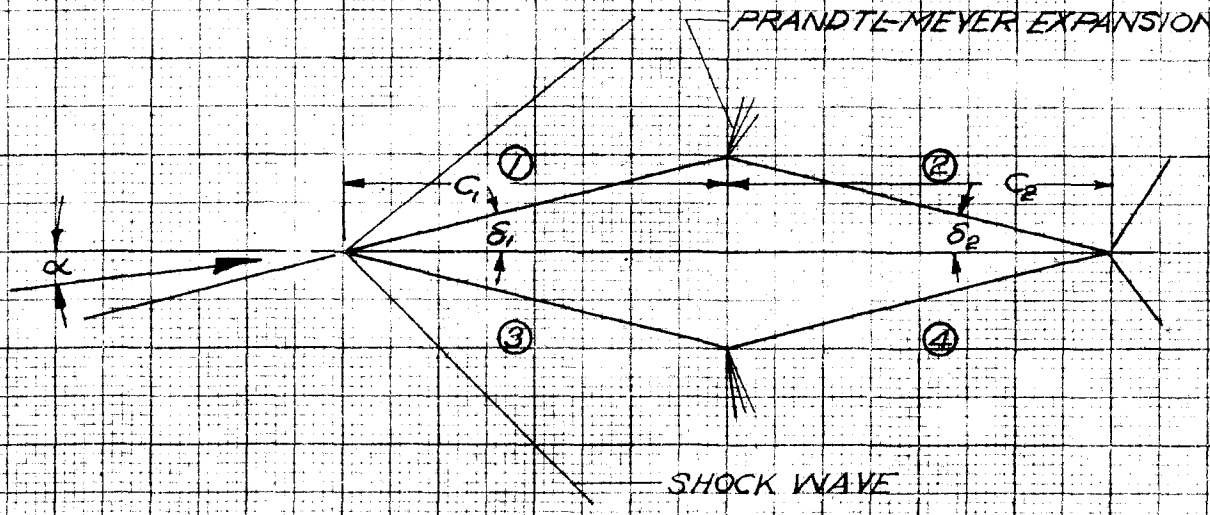

FIG. 1

DOUBLE WEDGE AIRFOIL

$$\theta_1 = \alpha - \delta_1$$
$$\theta_2 = \alpha + \delta_2$$
$$\theta_3 = \alpha + \delta_3$$
$$\theta_4 = \alpha - \delta_4$$

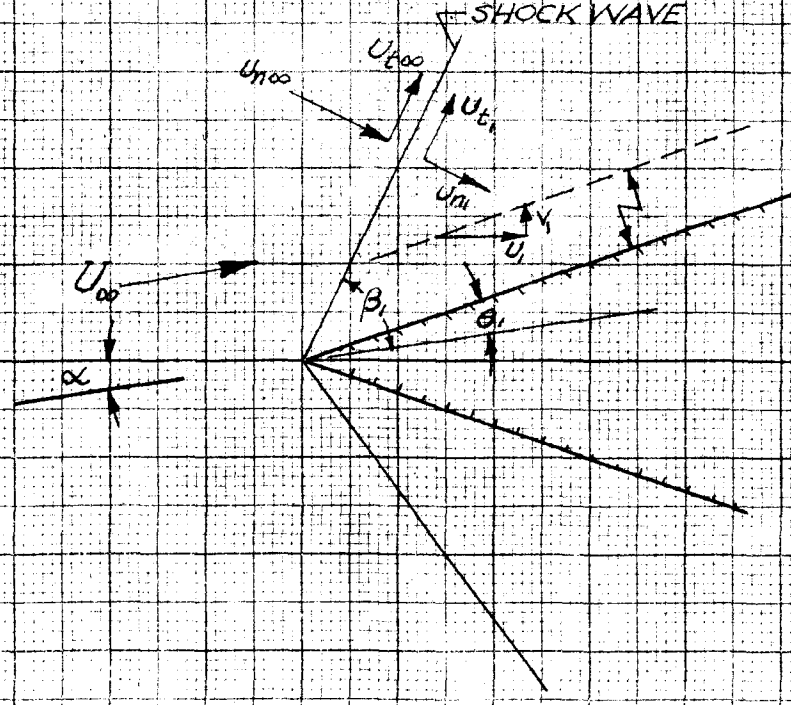

SHOCK WAVE NOTATION

FIG. 2

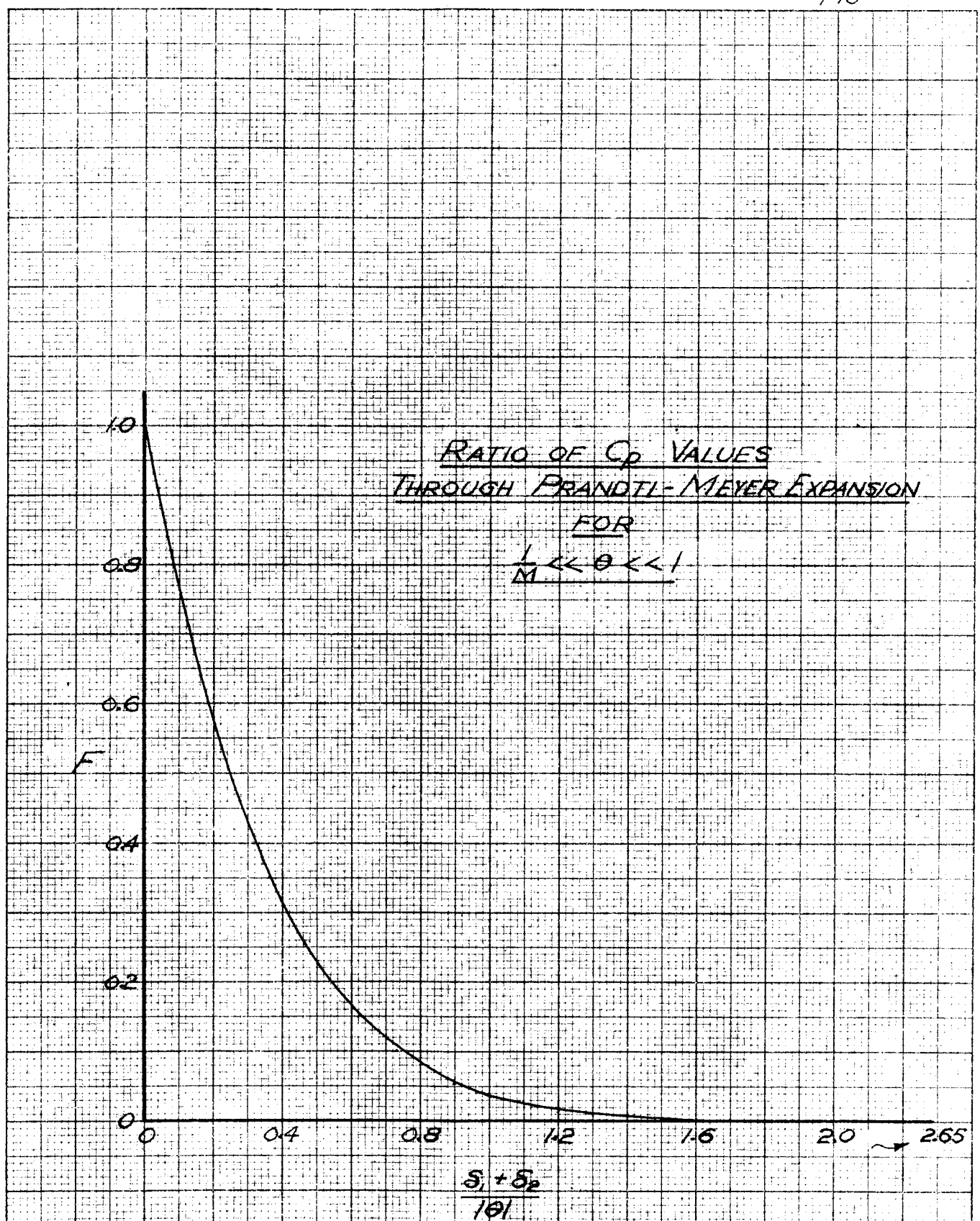
RATIO OF C_p VALUES
THROUGH PRANDTL-MEYER EXPANSION
FOR
$\frac{1}{M} << \theta << 1$
1.0
0.8
0.6
F
0.4
0.2
0
0
0.4
0.8
1.2
1.6
2.0
2.65
$\frac{S_1 + S_2}{101}$

FIG. 3

FIG. 4

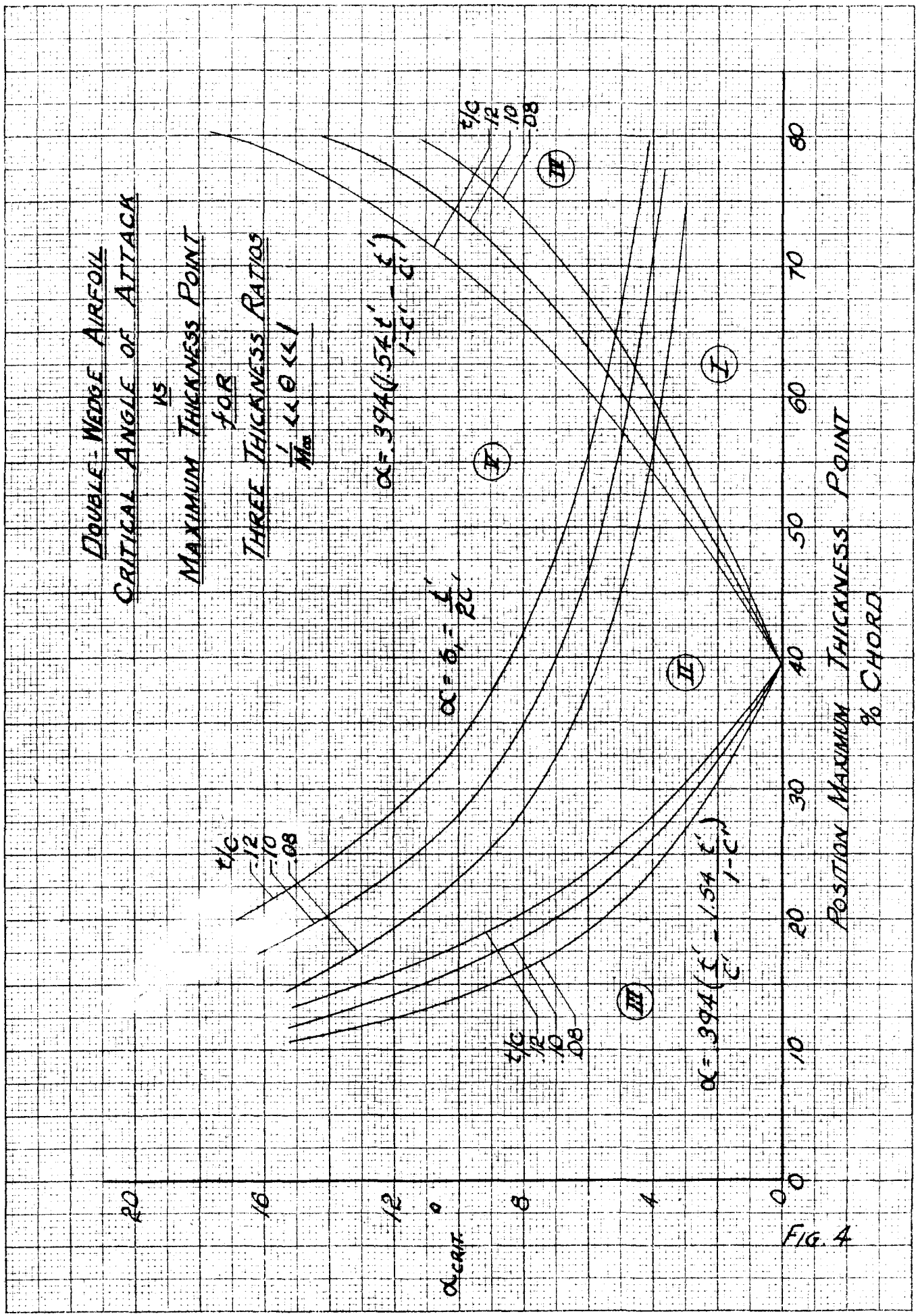
DOUBLE-WEDGE AIRFOIL
CRITICAL ANGLE OF ATTACK
VS
MAXIMUM THICKNESS POINT
FOR
THREE THICKNESS RATIOS
1/M∞ << θ << 1
t/c
.12
.10
.08
α = θ1 = t'/2c'
α = .394(1.54ζ' - ζ'²)/(1-c')
α = .394(ζ' - 1.54ζ'²)/(1-c')
I
II
III
IV
α CRIT °
0
4
8
12
16
20
0
10
20
30
40
50
60
70
80
POSITION MAXIMUM THICKNESS POINT
% CHORD

FIG. 4

FIG. 5

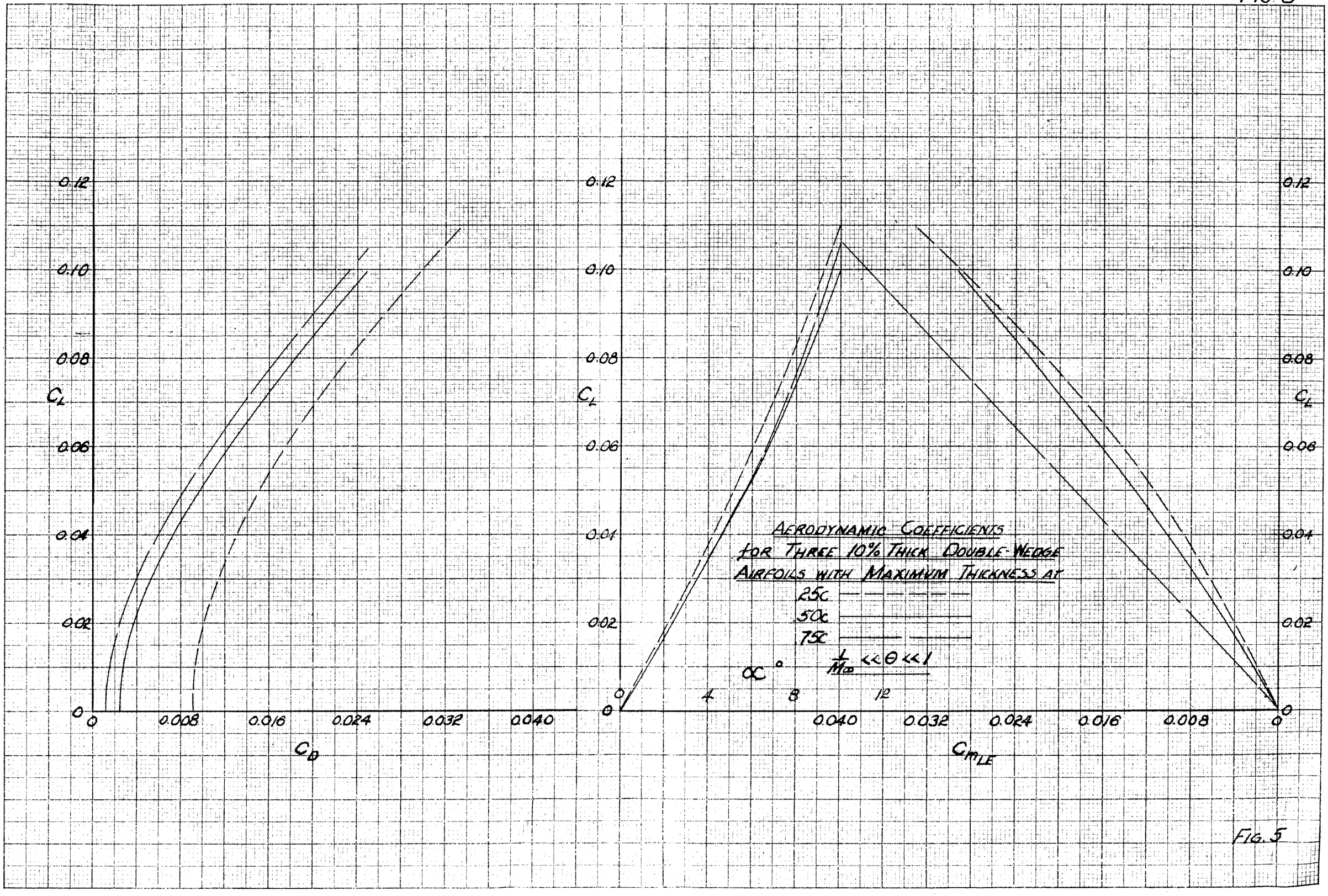
0.12
0.10
0.08
C_L
0.06
0.04
0.02
0
0
0.008
0.016
0.024
0.032
0.040
C_D
0.12
0.10
0.08
C_L
0.06
0.04
0.02
0
0
4
8
12
α°
$\frac{1}{M_\infty} << \theta << 1$
0.040
0.032
0.024
0.016
0.008
0
$C_{m_{LE}}$
AERODYNAMIC COEFFICIENTS
FOR THREE 10% THICK DOUBLE-WEDGE
AIRFOILS WITH MAXIMUM THICKNESS AT
.25c
.50c
.75c

FIG. 5

FIG. 6

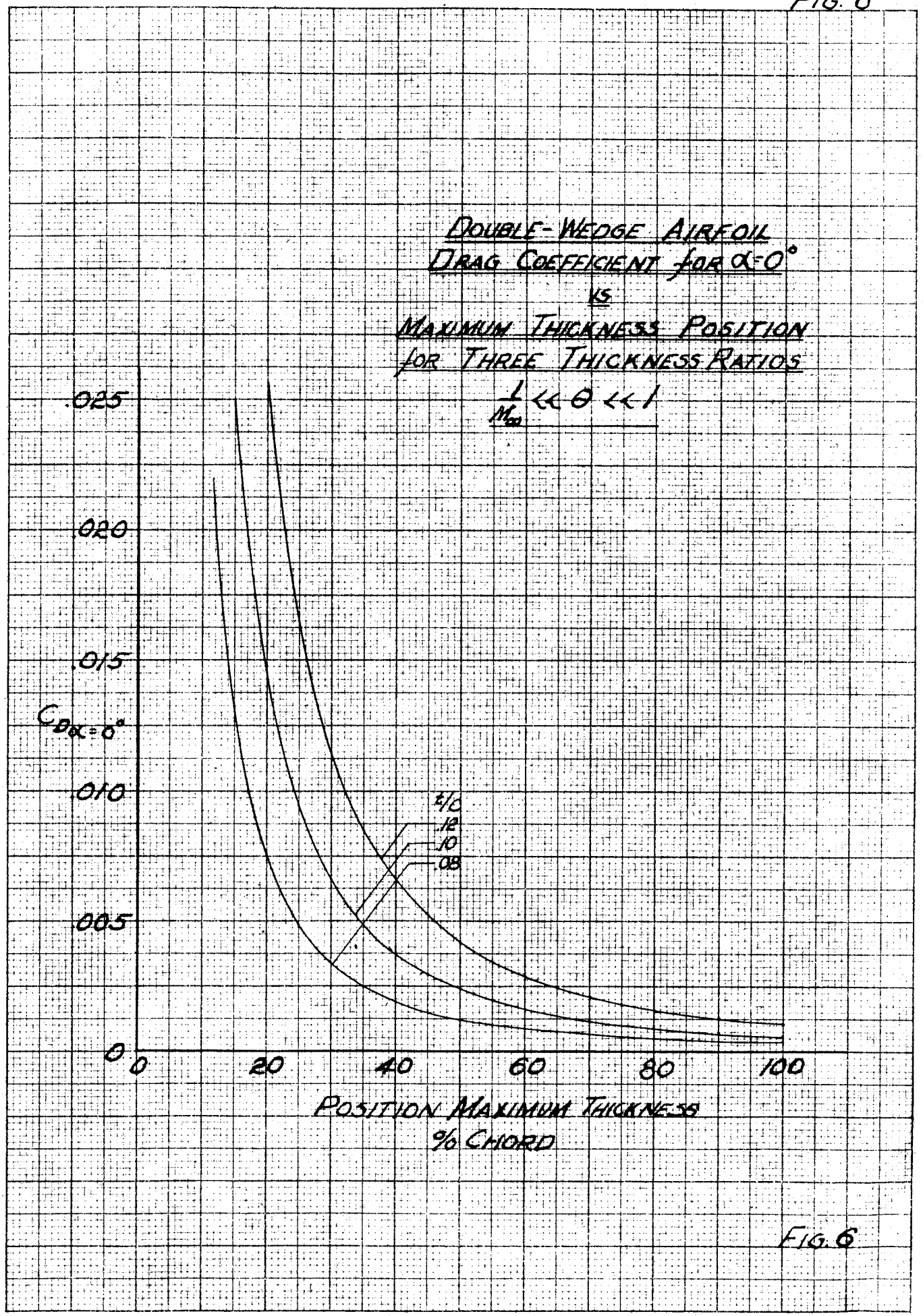
DOUBLE-WEDGE AIRFOIL
DRAG COEFFICIENT FOR α=0°
VS
MAXIMUM THICKNESS POSITION
FOR THREE THICKNESS RATIOS
1/M∞ << θ << 1
.025
.020
.015
.010
.005
0
$C_{D\alpha=0°}$
t/c
.12
.10
.08
0
20
40
60
80
100
POSITION MAXIMUM THICKNESS
% CHORD

FIG. 6

DOUBLE-WEDGE AIRFOIL
LIFT & MOMENT COEFFICIENT DERIVATIVES $\alpha=0°$
VS
POSITION OF MAXIMUM THICKNESS
FOR THREE THICKNESS RATIOS
$\frac{1}{M_\infty} << \beta << 1$

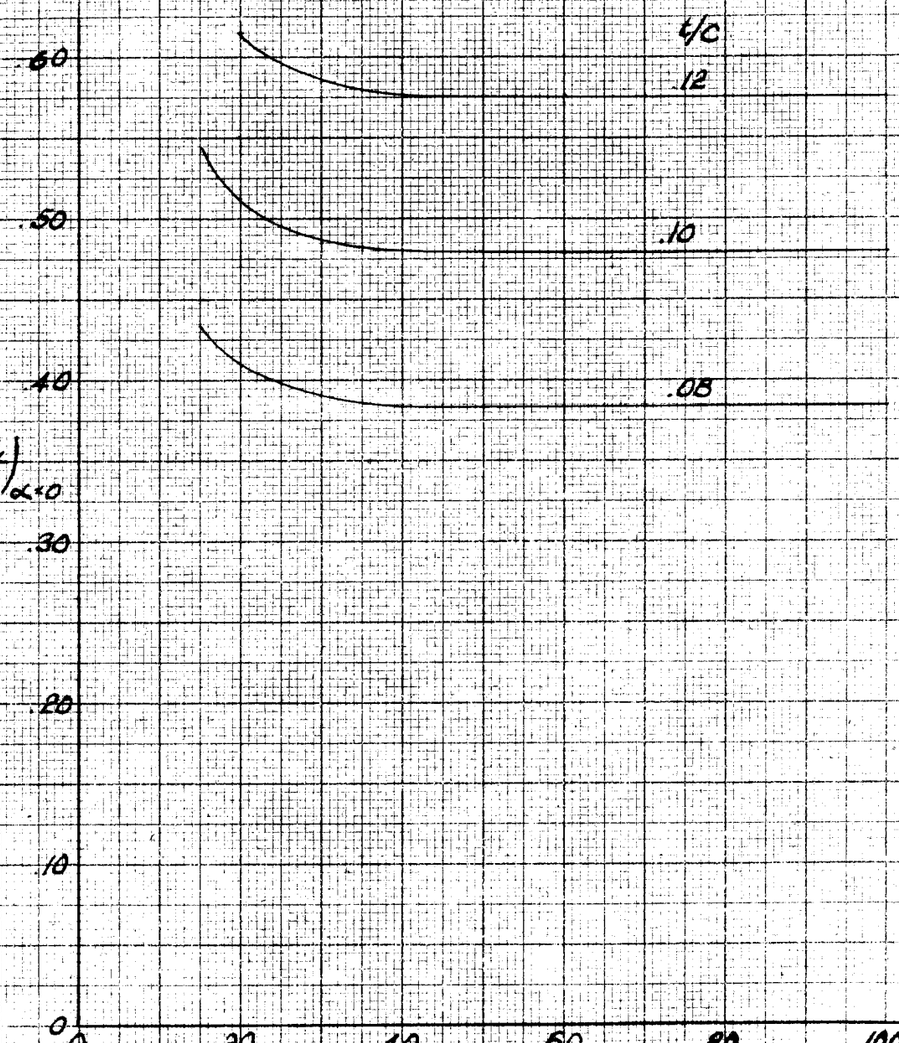

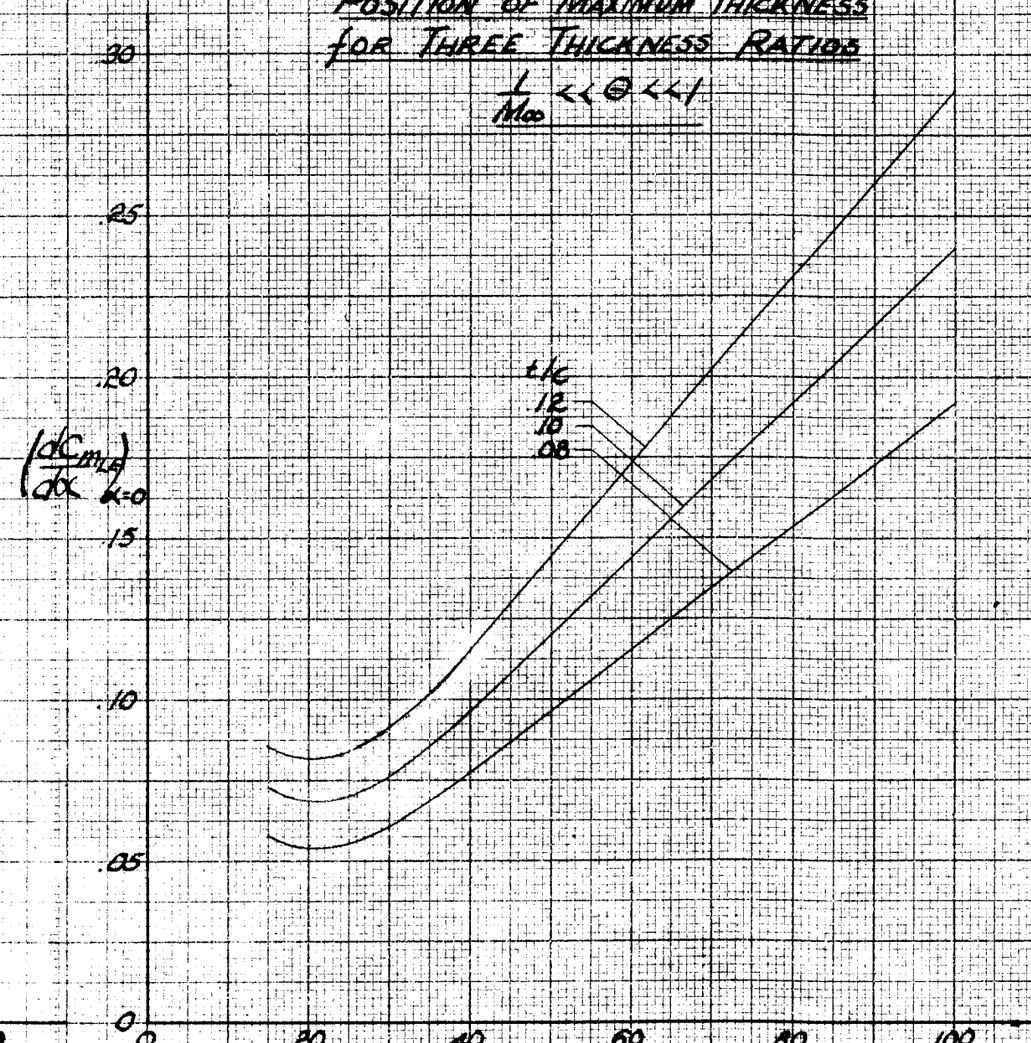

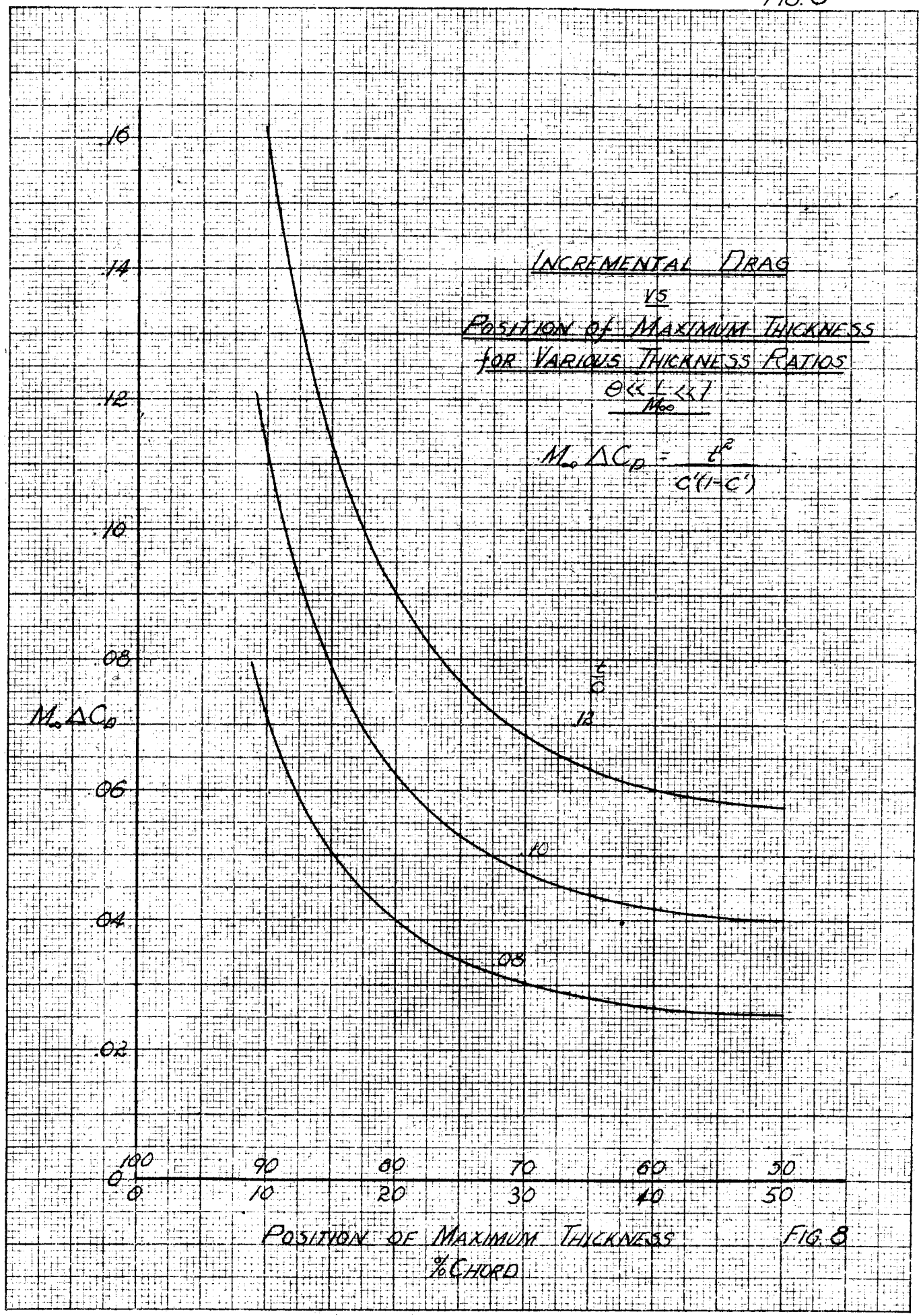
INCREMENTAL DRAG
VS
POSITION OF MAXIMUM THICKNESS
FOR VARIOUS THICKNESS RATIOS
$\theta \ll \frac{1}{M_\infty} \ll 1$
$M_\infty \Delta C_D = \frac{t^2}{C'(1-C')}$
$M_\infty \Delta C_D$
.16
.14
.12
.10
.08
.06
.04
.02
0
$\frac{t}{C}$
.12
.10
.08
100 90 80 70 60 50
0 10 20 30 40 50
POSITION OF MAXIMUM THICKNESS
%CHORD

FIG. 8

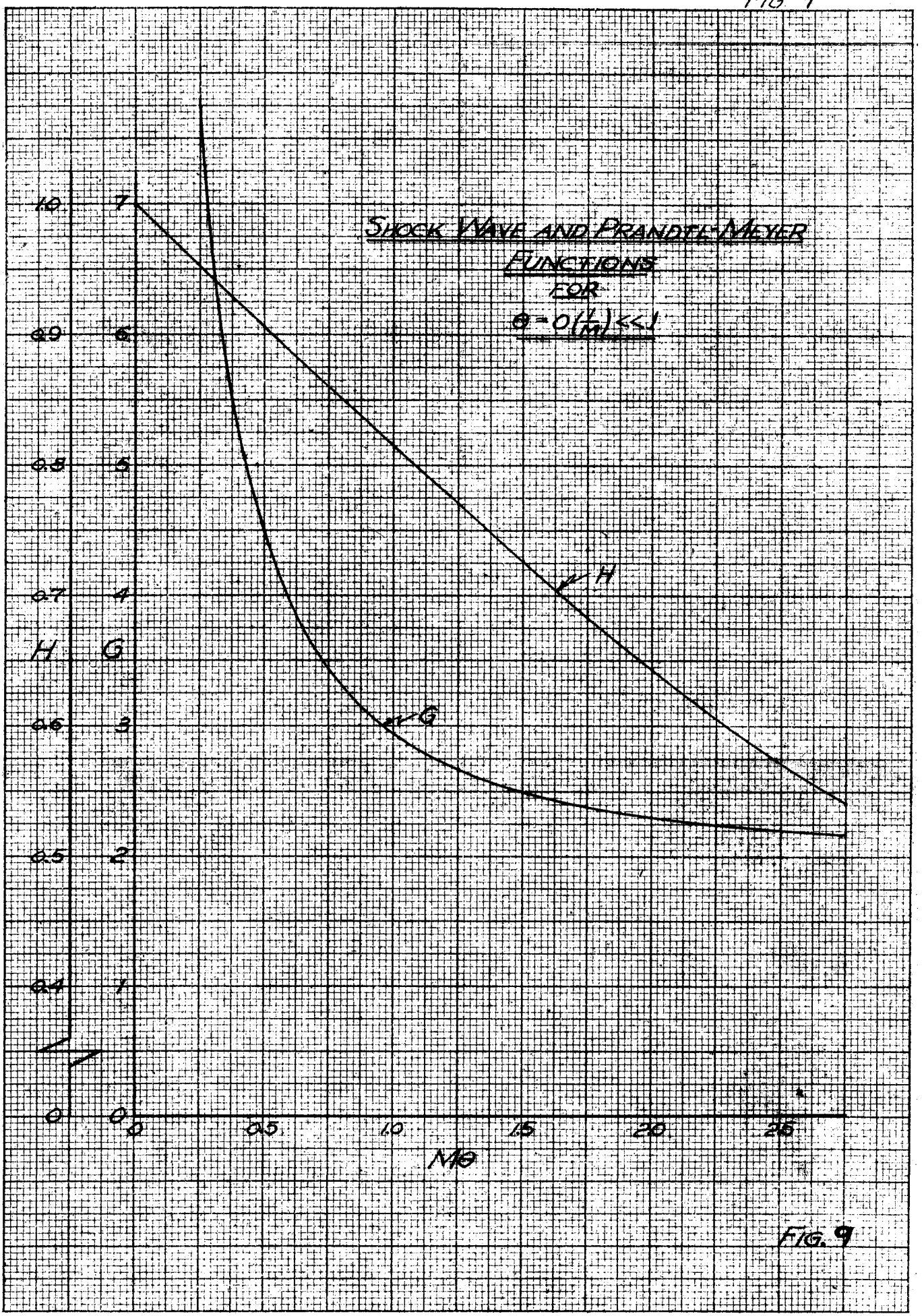
SHOCK WAVE AND PRANDTL-MEYER FUNCTIONS FOR
$\theta = O(\frac{1}{M}) << 1$
H
G
1.0
0.9
0.8
0.7
0.6
0.5
0.4
0
7
6
5
4
3
2
1
0
0
0.5
1.0
1.5
2.0
2.5
M_∞

FIG. 9

$\theta = O\left(\frac{t}{M_\infty}\right) << 1$

DOUBLE-WEDGE AIRFOIL
HYPERSONIC PRANDTL-MEYER FLOW CONDITIONS
FOR FLOW TO REJOIN THE
SURFACES
ANGLE OF ATTACK
VS
MAXIMUM THICKNESS POINT
FOR
THREE THICKNESS RATIOS
SURFACE ① LIMITING LINES

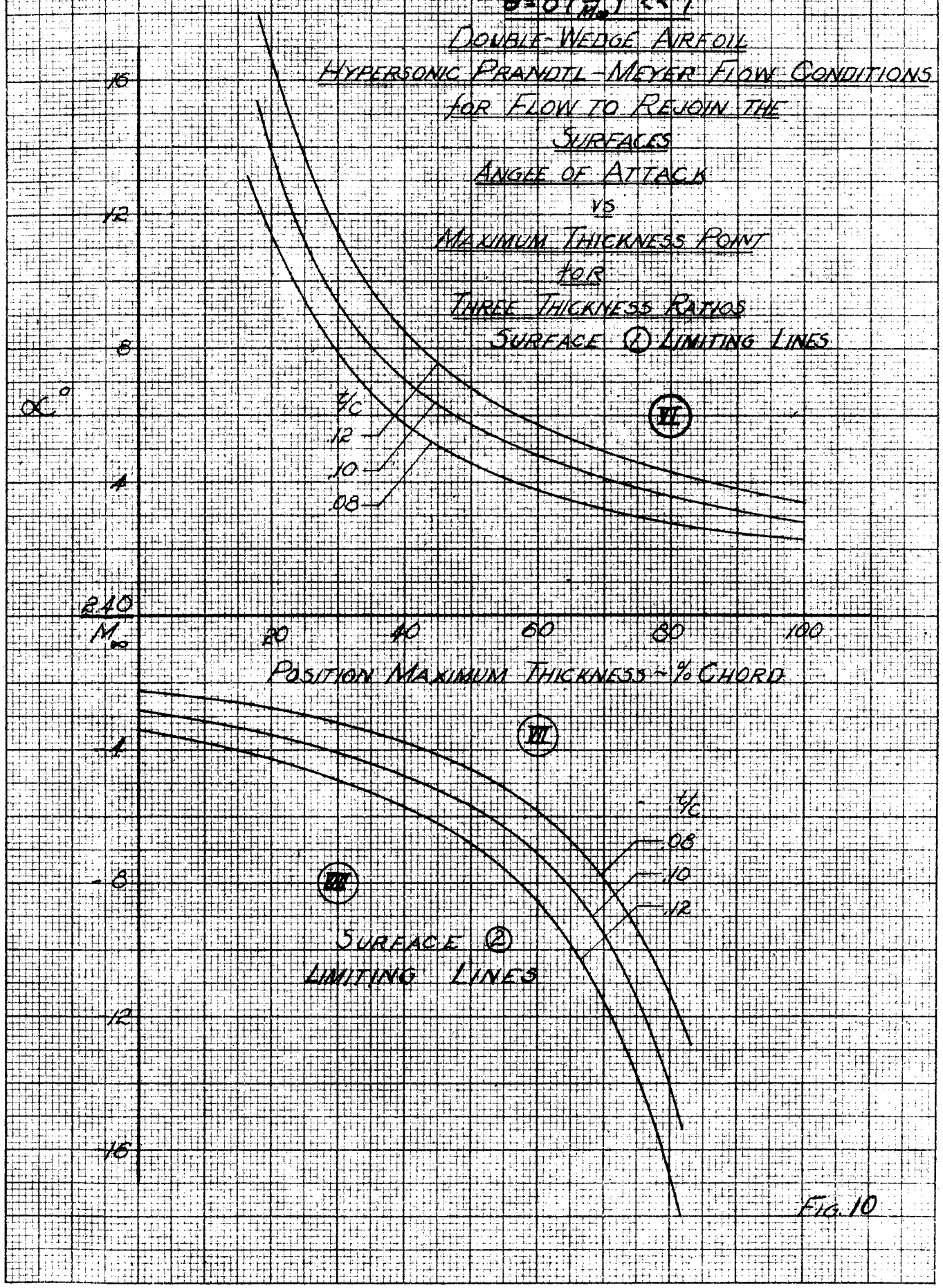

0.14
0.12
0.10
0.08
C_L
0.06
0.04
0.02
0
0 0.008 0.016 0.024 0.032 0.040
C_D

0.14
0.12
0.10
0.08
C_L
0.06
0.04
0.02
0
4 8 12 α°
0 0.008 0.016 0.024 0.032 0.040 0.048
$C_{m_{LE}}$

LINEARIZED THEORY

AERODYNAMIC COEFFICIENTS FOR THREE 10% THICK DOUBLE WEDGE AIRFOILS WITH MAXIMUM THICKNESS AT
.25c
.50c
.75c
$\theta = O(\frac{t}{c})$ KK 1, $M_\infty = 1.0$

FIG. 11

FIG. 12

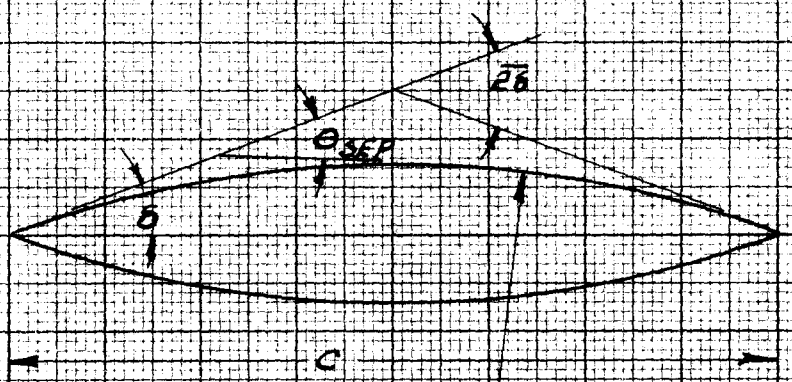

BICONVEX AIRFOIL NOTATION

q

FIG. 12

BICONVEX AIRFOIL

LIMITING LINES FOR C_L (100), C_D (103), $C_{m_{LE}}$ (105)

CRITICAL ANGLE OF ATTACK RATIO

VS

SEPARATING ANGLE RATIO

$\frac{1}{M_\infty} \ll \Theta \ll 1$

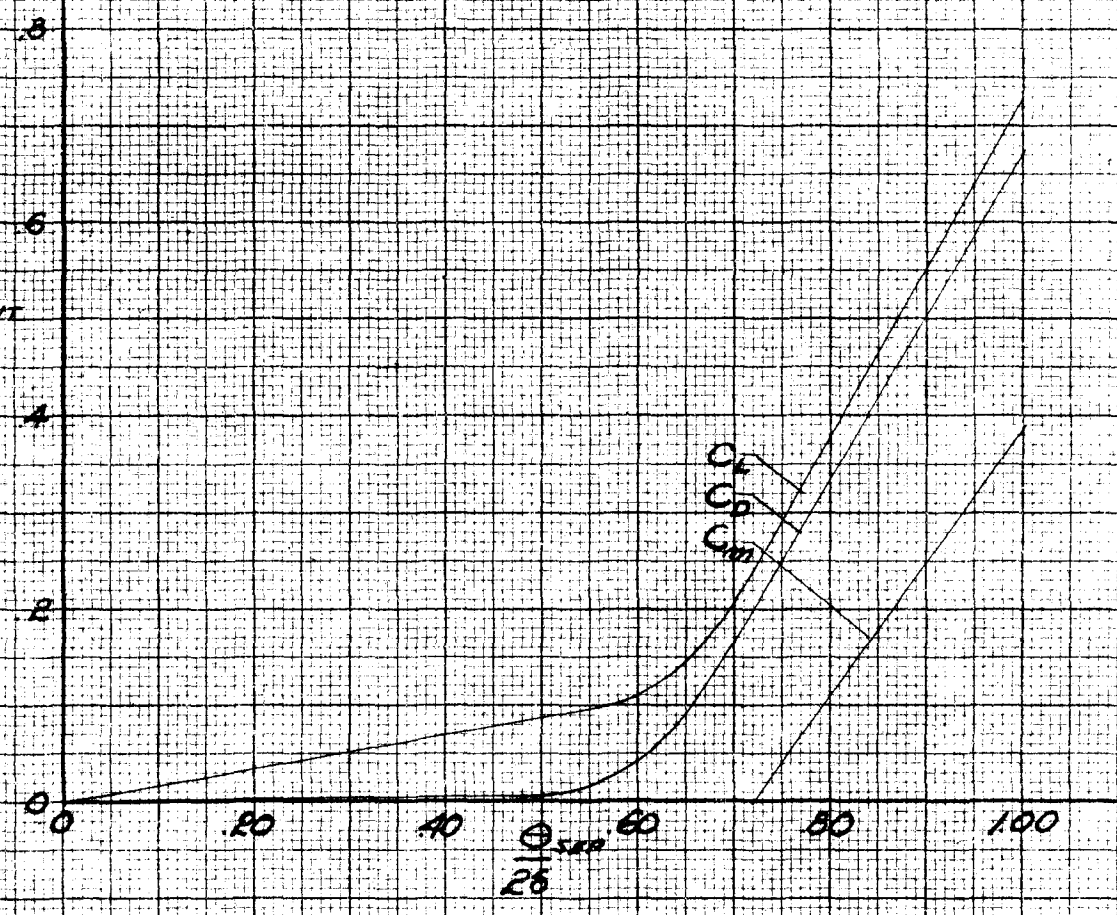

FIG. 13